R. & M. No. 3377

MINISTRY OF AVIATION

AERONAUTICAL RESEARCH COUNCIL
REPORTS AND MEMORANDA

Inflated Mobile Lifting Structures: Analysis of Generator-Cord Construction for Circular Planforms

By W. G. S. Lester, M.A., D.Phil.

LONDON: HER MAJESTY'S STATIONERY OFFICE
1964
PRICE 18*s.* 6*d.* NET

Inflated Mobile Lifting Structures: Analysis of Generator-Cord Construction for Circular Planforms

By W. G. S. Lester, M.A., D.Phil.

Communicated by the Deputy Controller Aircraft (Research and Development), Ministry of Aviation

*Reports and Memoranda No. 3377**

July, 1962

Summary.

An inflatable lifting system basically consists of a flexible membrane attached to the periphery of a base containing an orifice. A load is suspended from the inner surface of the membrane and the base rests in contact with the ground; on inflating the device the load is raised and with suitable design and a continuous pressure supply the structure can lose ground contact and hover. An equilibrium configuration is said to have been reached when air is about to escape from the base orifice and ground contact is lost.

A model of a system is considered in which the load is carried in a set of cords attached to the periphery of an annular base. These cords are shorter than the length of fabric gore which lies between them and bows outwards under the excess pressure. The statics of the structure are analysed and it is shown that for practical design purposes the base orifice area should be less than half the projected area of the canopy below the load suspension points. Possible equilibrium configurations are investigated and a method for calculating the fabric gore shape is given. Formulae for designing an actual system are included.

LIST OF CONTENTS

* Replaces R.A.E. Tech. Note No. Mech. Eng. 356—A.R.C. 24 501.

LIST OF APPENDICES

LIST OF TABLES

LIST OF ILLUSTRATIONS

---

1. *Introduction.*

The general concept of an inflatable lifting system can be understood by considering a flexible imporous membrane which is attached to the periphery of a base; this base, which may be regarded as rigid, is in the form of a disc with either a single orifice or an array of several orifices. For a completely collapsible structure the base is assumed to obtain its rigidity by means of, for example, inflated fabric ribs. A load mass is attached to points on the inner surface of the membrane by a series of cords. A mechanical unit is provided to inflate the system and when the pressure difference between the region interior to the membrane and the atmosphere is sufficient the load is lifted from the plane and supported by tensions in the fabric structure. On further increasing the pressure the system takes up some characteristic shape and a stage is reached where air commences to escape from the base orifice(s); by using a continuous air supply the whole structure can be made to leave the plane and hover. The position in which air is about to escape from the base orifice is regarded in this report as the equilibrium position. Whilst the load is being raised to this so-called equilibrium position and the base is still in contact with the plane there must be a ground reaction on the base; once the system loses physical contact with the plane this reaction is zero.

This report is concerned with the equilibrium configuration of the structure when air is about to escape from the base orifice and the system loses contact with the plane; its object is to determine the shape taken up by the membrane and, if possible, to specify the optimum position for the cords supporting the load. The attraction of devices of this nature rests in their ability to raise a load of, say, 10,000 lb with a pressure difference of the order of $0{\cdot}1$ atmospheres or less. The system does not always work as intended: sometimes air escape occurs before the load has even been raised, or the base buckles and adequate pressurisation is impossible. In consequence, it is

desirable to provide some theoretical guide to design procedure for the basic structure: as a tentative approach to the problem a particular model is considered, based on the theoretical model for the parachute with cords over the canopy[1], which, although possibly unrepresentative of devices which have been constructed, is amenable to an approximate theoretical analysis and may assist in the formulation of a more generally applicable theory.

Some brief observations are made in Appendices on the events occurring from the start of inflation to the attainment of the equilibrium configuration and on a higher approximation to the theory.

It should be remarked that the report is not concerned with the dynamical problems involved once ground contact is lost and air escape occurs.

2. *The Model.*

The base for the structure is assumed to be a circular annular hoop of outer radius R_1 and inner radius b; this does not imply that the analysis only applies to a structure with a single circular base orifice, it is valid for any arrangement of orifices having an area equivalent to that of the circle of radius b, i.e. πb^2. However, where several orifices are employed they must be suitably arranged to maintain stability and symmetry and allow for control of the device when hovering. Attached at each of n points at equal intervals around the outer circumference of the base is a cord of length L, where L is greater than R_1; these cords are referred to as generator cords and their ends are joined together to form an apex at O. At a distance s_1 from O along each of the generator cords, is attached another cord of length l, referred to as a load cord, and these cords are attached to the load mass M. The surface regions between the generator cords and the outer circumference of the base are spanned by imporous fabric, the load cords passing through seals in the fabric, so that when the base is resting on a plane and the generator cords are fully extended, as if the system were suspended from the apex O, the configuration resembles a conical shell. For the present it is assumed that the shape of the fabric lying between adjacent generator cords, i.e. the gore shape, is undefined but there is a certain fullness in this fabric and it is gathered along the generator cords and can billow between them. The fabric, generator and load cords are all assumed to be inextensible and to have no flexural rigidity.

When a positive pressure difference occurs between the inner region of the fabric shell and the atmosphere the generator cords take up a characteristic shape and the gore fabric bulges outwards between them. With a sufficiently high pressure differential and suitable geometry the load is raised from the plane and the final configuration may resemble that shown in Fig. 1(i). A sectionalised three-dimensional view is shown in Fig. 1(ii).

It is assumed that the whole of the load is carried by the tensions in the generator cords and that the fullness of the gore fabric is such that only circumferential tension, which is assumed constant over the length of a gore, exists in it. Physically there must be some generator tension in the fabric gores, but gathering along the generator cords relieves this and it is to be expected that the generator tension can be made very small in comparison with the circumferential tension.

The masses of the canopy, load cords and base are assumed negligible in comparison with the mass of the load; but, if a heavy base is used, account should be taken of this and the basic equations suitably modified.

The fabric region above the points of suspension of the load cords is called the upper canopy and the region between these points and the base is the lower canopy. The pressure difference

across the whole of the canopy's surfaces and the base is assumed constant and equal to p; this assumption is reasonable before air escape occurs but may not be adequate once the structure leaves the ground, discussion of this situation is outside the scope of the present report.

In Fig. 1 a point load is shown suspended by the cords attached to the suspension points, this involves some bracing of the structure. The same configuration could theoretically be attained by distributing the load uniformly around the suspension-point interface in the form of a ring of radius r_1, or as point loads Mg/n acting at each of the suspension points; in the latter case it would be necessary to connect radially opposite suspension points by cords in order to brace the structure.

3. *Theory of the System.*

Let the tension in the upper-canopy generator cords be T_1; in the lower-canopy cords T_2; and in each load cord F. The lower-canopy generator cords leave the base at an angle δ with the plane, as shown in Fig. 1, and in consequence there is a radial tension T_3 in the base to balance the horizontal component of the generator-cord tension. Vertical distance x is measured downwards from O or O′ and the radial co-ordinate from this vertical axis is r. The maximum distance of the upper-canopy cords from the axis is a and of the lower-canopy cords is R; the radius of the suspension-point interface is r_1. The total arc length from a suspension point A to O, the apex, is s_1 and from A to C a point on the base, is s_2. The tangent to the upper-canopy cords makes an angle ψ with Or and the tangent to the lower cords an angle φ. At A the upper-canopy cord makes an angle α with the horizontal and the lower-canopy cord an angle β; the load cord for a point load is inclined at γ to the horizontal. Fig. 1(i) as drawn shows the angle β measured counterclockwise and positive; this is for convenience in the analysis. In practice a positive β is undesirable since the tension in the lower canopy is then tending to pull the load down rather than raise it. It is normally expected that β will be negative for an efficient system and to this extent Fig. 1(i) represents an impractical design.

For the arc length from O to C:

$$s_1 + s_2 = L. \tag{1}$$

For the upper canopy, neglecting the additional projected area due to bowing out of the gore:

$$p\pi a^2 = nT_1. \tag{2}$$

For the suspension-point interface:

$$nT_1 \sin\alpha - nT_2 \sin\beta = nF \sin\gamma = Mg. \tag{3}$$

For the whole system:

$$p\pi b^2 = Mg. \tag{4}$$

For the lower canopy, again neglecting the added area due to bowing out of the gore, and using equation (4):

$$p\pi R^2 - Mg = nT_2 = p\pi(R^2 - b^2). \tag{5}$$

For the base:

$$p\pi(R_1^2 - b^2) = nT_2 \sin\delta. \tag{6}$$

$$T_3 = T_2 \cos\delta. \tag{7}$$

These equations only apply when air is about to escape and the ground reaction is zero: Appendix III deals with the situation occurring before full inflation and Appendix IV gives the theory including the effect of additional projected area due to bowing out of the gore fabric.

3.1. *The Upper Canopy.*

The equilibrium of the fabric between two planes corresponding to $x = x$ and $x = x + \delta x$ is considered. For an element of generator cord δs the outward pressure forces must balance the tension. The tension in the fabric where it meets the generator cord is everywhere at right angles to the cord and so the tension in the cord is constant over its length.

Referring to Fig. 2, which represents a section of the upper canopy:

$$T_1 \sin \delta\psi \doteq p \frac{2\pi r}{n} \delta s$$

or, in the limit:

$$T_1 \delta\psi = p \frac{2\pi r}{n} \delta s . \tag{8}$$

Also

$$\delta r = \delta s \cos \psi . \tag{9}$$

Now

$$\frac{d\psi}{dr} = \frac{\delta\psi}{\delta s} \frac{\delta s}{\delta r} = p \frac{2\pi r}{n T_1} \frac{1}{\cos \psi}$$

and using (2):

$$\cos \psi \frac{d\psi}{dr} = \frac{2r}{a^2} . \tag{10}$$

The integration of (10) gives

$$[\sin \psi]_{\psi_0}^{\psi} = \left[\frac{r^2}{a^2}\right]_{r_0}^{r} ;$$

but

$$r_0 = a \qquad \text{when} \qquad \psi_0 = \frac{\pi}{2} \qquad \text{and}$$

therefore

$$\sin \psi = \frac{r^2}{a^2} \tag{11}$$

which gives the equation of the upper-canopy generator cords. This equation (11) represents the well-known Taylor shape.

At the suspension points A:

$$r = r_1 \qquad \text{and} \qquad \psi = \pi - \alpha ,$$

hence

$$r_1^2 = a^2 \sin \alpha . \tag{12}$$

3.2 *The Lower Canopy.*

Similarly for the lower-canopy generator cords

$$T_2 \delta\varphi = p \frac{2\pi r}{n} \delta s \tag{13}$$

$$\delta r = \delta s \cos \varphi \tag{14}$$

and using (5):

$$\cos \varphi \frac{d\varphi}{dr} = \frac{2r}{R^2 - b^2} .$$

Intregrating this

$$[\sin \varphi]_{\varphi_0}^{\varphi} = \left[\frac{r^2}{R^2 - b^2}\right]_{r_0}^{r}.$$

When

$$\varphi_0 = \beta, \quad r_0 = r_1 = +(a^2 \sin \alpha)^{1/2};$$

therefore

$$\sin \varphi - \sin \beta = \frac{r^2 - a^2 \sin \alpha}{R^2 - b^2}. \tag{15}$$

When

$$\varphi = \frac{\pi}{2}, \quad r = R;$$

therefore

$$(R^2 - b^2) \sin \beta = a^2 \sin \alpha - b^2. \tag{16}$$

Thus, from (15) and (16),

$$\sin \varphi = \left(\frac{r^2 - b^2}{R^2 - b^2}\right) \tag{17}$$

which gives the equation of the lower-canopy generator cords.

4. *Geometric Parameters for the System.*

The equations of the upper- and lower-canopy generator cords enable the arc lengths and vertical co-ordinates of the system to be calculated. For the upper canopy:

$$\frac{r^2}{a^2} = \sin \psi \qquad \text{and} \qquad ds = \frac{dr}{\cos \psi}$$

whence

$$s = \frac{a}{2} \int_0^{\psi} \frac{d\psi}{\sqrt{\sin \psi}} \tag{18}$$

and the total arc length s_1 from O to A is given by

$$\frac{s_1}{a} = \frac{1}{2} \int_0^{\pi - \alpha} \frac{d\psi}{\sqrt{\sin \psi}}. \tag{19}$$

For the vertical co-ordinate x, measured from O:

$$dx = \tan \psi dr$$

and hence

$$x = \frac{a}{2} \int_0^{\psi} \sqrt{\sin \psi} d\psi \tag{20}$$

and the height of the upper canopy alone is given by

$$\frac{x_1}{a} = \frac{1}{2} \int_0^{\pi - \alpha} \sqrt{\sin \psi} d\psi. \tag{21}$$

Similarly for the lower canopy where

$$\sin \varphi = \frac{r^2 - b^2}{R^2 - b^2},$$

$$s = \int_{\beta}^{\varphi} \frac{(R^2 - b^2) d\varphi}{2\sqrt{\{(R^2 - b^2) \sin \varphi + b^2\}}}. \tag{22}$$

Setting

$$b = \mu R \qquad \text{where} \qquad 0 < \mu \leqslant 1 \tag{23}$$

the total arc length s_2 from A to C is given by

$$\frac{s_2}{R} = \frac{1}{2}\int_{\beta}^{\pi-\delta} \frac{(1-\mu^2)d\varphi}{\sqrt{\{(1-\mu^2)\sin\varphi + \mu^2\}}}. \tag{24}$$

For the vertical co-ordinate x, measured from O′:

$$\frac{x}{R} = \frac{1}{2}\int_{\beta}^{\varphi} \frac{(1-\mu^2)\sin\varphi d\varphi}{\sqrt{\{(1-\mu^2)\sin\varphi + \mu^2\}}} \tag{25}$$

and the height of the lower canopy is

$$\frac{x_2}{R} = \frac{1}{2}\int_{\beta}^{\pi-\delta} \frac{(1-\mu^2)\sin\varphi d\varphi}{\sqrt{\{(1-\mu^2)\sin\varphi + \mu^2\}}}. \tag{26}$$

The integrals involved in (18) to (26) are all elliptic and their reduction to standard forms and evaluation is given in Appendix I.

4.1. *A Criterion for a Possible Equilibrium Configuration.*

Consider the equation for the lower generator cords:

$$\sin\varphi = \frac{r^2 - b^2}{R^2 - b^2}.$$

Now r is always real and positive and

$$|\sin\varphi| \leqslant 1;$$

hence

$$\left|\frac{r^2 - b^2}{R^2 - b^2}\right| \leqslant 1,$$

or

$$\left|1 - \frac{R^2 - r^2}{R^2 - b^2}\right| \leqslant 1,$$

therefore

$$0 \leqslant \frac{R^2 - r^2}{R^2 - b^2} \leqslant 2.$$

With $b = \mu R$ and $0 < \mu \leqslant 1$ this becomes

$$0 \leqslant R^2 - r^2 \leqslant 2(1-\mu^2)R^2$$

or

$$r^2 \geqslant (2\mu^2 - 1)R^2.$$

For it to be possible to make a system consisting of a lower canopy only with a single suspension point at the apex this inequality must be valid for *all* $r \leqslant R$ and can then only be satisfied if

$$2\mu^2 - 1 \leqslant 0. \tag{27}$$

Hence, in these circumstances, before an equilibrium configuration can exist it is essential that

$$0 < b \leqslant \frac{R}{\sqrt{2}}. \tag{28}$$

This implies that with a single-point suspension the maximum load which can be lifted is

$$Mg = p\pi b^2 \leqslant p\frac{\pi R^2}{2}, \tag{29}$$

but this, as shown in Section 4.3, is practically somewhat lower. Thus, for a given maximum lower-canopy radius R and pressure difference p, the maximum load is specified by the limitations on b. The effective maximum lifting surface of the system is equal to half the maximum projected area of the lower canopy. For a system to be designed to carry a load from multiple points and also to be usable with single-point suspension the relations (28) and (29) must still be applied.

If a system is only required to carry a load from a number of points and a possible single-point suspension is excluded, the restriction (27) on the value of μ no longer applies. Instead it is essential to have an upper canopy with the radius at the suspension-point interface satisfying the inequality

$$\left(\frac{r_1}{R}\right)^2 \geqslant 2\mu^2 - 1.$$

This situation presents some difficulties for it will be shown that when μ is larger than say 0·6 to 0·7 the lower canopy becomes very squat and may not be high enough to accommodate the load beneath the suspension points. To overcome this it appears that for large values of μ the load would have to be cantilevered from the suspension points to get it clear of the ground. It is questionable whether this is of practical value.

In general the ensuing analysis applies only to the cases where $0 < \mu \leqslant 1/\sqrt{2}$ and single-point suspension is possible. Appendix V considers the problem with $\mu > 1/\sqrt{2}$; separate consideration is necessary since the integrals (24) to (26) for the arc length and height of the lower canopy lead to different results in general, depending whether μ is greater or less than $1/\sqrt{2}$.

Further limitations on the value of μ arise in Section 4.3 where the height of the suspension points above the ground is considered, and the more accurate analysis of Appendix IV shows that the restrictions on μ can be slightly relaxed. The practical limit for μ however appears to be largely unchanged when the limits of the theory are borne in mind.

4.2. *Determination of the Configuration of the System with* $\mu < 1/\sqrt{2}$.

In order for the configuration of the system to be determinate the values of some of the geometric parameters involved must be specified. Suppose, for example, that the given factors are the annular base radii, R_1 and b; the maximum radius of the lower canopy R; and the two arc lengths s_1 and s_2: a knowledge of these factors is sufficient to determine the resulting configuration of the whole system. From equations (19) and (24):

$$s_1 = s_1(a, \alpha)$$

$$s_2 = s_2(R, b, \beta, \delta);$$

from equation (16):

$$\beta = \beta(R, a, b, \alpha);$$

and from equation (17):

$$\delta = \delta(R_1, R, b).$$

These four equations involve the four unknowns α, β, δ, and a and the problem is determinate. The solution of the equations is a rather cumbersome though straightforward process involving

the use of tabulated values of elliptic integrals. When α, β, δ and a have been determined it is possible to calculate the vertical co-ordinates, x, for the system, and the radial co-ordinates r, thus enabling the configuration to be plotted graphically. For a given load the required pressure can be obtained from equation (4) and the resulting tensions in the generator cords and base hoop from equations (2) to (7).

To discuss possible equilibrium configurations the results obtained in Appendix I for the geometric parameters of Section 4 are required and a summary and discussion of these results follows.

For the arc length of the upper canopy measured from O to some point on the generator cord with co-ordinate ψ:

$$\frac{s}{a} = \frac{1}{\sqrt{2}} F\left(\frac{\pi}{2}, \frac{1}{\sqrt{2}}\right) - \frac{1}{\sqrt{2}} F\left(\theta, \frac{1}{\sqrt{2}}\right) \tag{30}$$

where

$$\theta = \cos^{-1}(\sqrt{\sin\psi}) \tag{31}$$

and the total arc length s_1 is given by putting $\psi = \pi - \alpha$. Now the maximum value for ψ is $\pi - \alpha$ and α can take values such that

$$0 < \alpha < \pi,$$

when α is measured in a clockwise direction as in Fig. 1(i); an increase in s_1 thus results in a decrease in α. The corresponding range for θ may be taken as

$$-\frac{\pi}{2} \leqslant \theta \leqslant \frac{\pi}{2},$$

where $\theta = -\pi/2$ corresponds to $\alpha = 0$ and $\theta = +\pi/2$ corresponds to $\alpha = \pi$. Depending on the angle α the upper canopy is either a section of the curve taken by a plane which lies above the plane containing $r = a$, or a section by a plane lying below that containing $r = a$. These two sections are shown in Figs. 3(i) and (ii).

For the vertical co-ordinate of the upper canopy the result obtained is:

$$\frac{x}{a} = \sqrt{2}\, E\left(\frac{\pi}{2}, \frac{1}{\sqrt{2}}\right) - \sqrt{2}\, E\left(\theta, \frac{1}{\sqrt{2}}\right) - \frac{1}{\sqrt{2}} F\left(\frac{\pi}{2}, \frac{1}{\sqrt{2}}\right) + \frac{1}{\sqrt{2}} F\left(\theta, \frac{1}{\sqrt{2}}\right) \tag{32}$$

where the range corresponding to $0 < \psi < \pi$ is

$$-\frac{\pi}{2} < \theta < \frac{\pi}{2}.$$

For the lower canopy s is measured from A to some point on the generator cord with co-ordinate φ, where φ has a maximum value of $\pi - \delta$ and a minimum value of β, where β may be negative. If there is no upper canopy at all the minimum value of β occurs when $r = 0$ and then

$$\beta = \sin^{-1}\left(-\frac{\mu^2}{1-\mu^2}\right). \tag{33}$$

Even with an upper canopy β is still negative where $r < b$. These cases are illustrated in Figs. 4 and 5.

The arc length s for the lower canopy is given by

$$\frac{s}{R} = \frac{\sqrt{(1-\mu^2)}}{\sqrt{2}} F\left(\xi_1, \frac{1}{\sqrt{\{2(1-\mu^2)\}}}\right) - \frac{\sqrt{(1-\mu^2)}}{\sqrt{2}} F\left(\xi, \frac{1}{\sqrt{\{2(1-\mu^2)\}}}\right), \tag{34}$$

where

$$\xi_1 = \cos^{-1}\sqrt{\{(1-\mu^2)\sin\beta + \mu^2\}} \tag{35}$$

and

$$\xi = \cos^{-1}\sqrt{\{(1-\mu^2)\sin\varphi + \mu^2\}}. \tag{36}$$

For $-\pi/2 \leqslant \varphi \leqslant \pi/2$, ξ must be taken to lie in the range $\pi/2 \geqslant \xi \geqslant 0$ where $\xi = 0$ corresponds to $\varphi = \pi/2$ and $\xi = \pi/2$ corresponds to $\varphi = \sin^{-1}\{\mu^2/(1-\mu^2)\}$. When $\varphi \geqslant \pi/2$, ξ lies in the range $0 \geqslant \xi \geqslant -\pi/2$ where $\xi = 0$ corresponds to $\varphi = \pi/2$ and $\xi = -\pi/2$ corresponds to $\varphi = -\sin^{-1}\{\mu^2/(1-\mu^2)\} + \pi$. The total arc length s_2 from A to C is given by equation (34) with $\varphi = \pi - \delta$.

The vertical co-ordinate x, measured downwards from A, for the lower canopy, is given by

$$\frac{x}{R} = \sqrt{\{2(1-\mu^2)\}}\left[E\left(\xi_1, \frac{1}{\sqrt{\{2(1-\mu^2)\}}}\right) - E\left(\xi, \frac{1}{\sqrt{\{2(1-\mu^2)\}}}\right)\right] -$$

$$- \frac{\sqrt{(1-\mu^2)}}{\sqrt{2}}\left[F\left(\xi_1, \frac{1}{\sqrt{\{2(1-\mu^2)\}}}\right) - F\left(\xi, \frac{1}{\sqrt{\{2(1-\mu^2)\}}}\right)\right] \tag{37}$$

with the corresponding ranges of ξ and φ as for the arc length s. Now from equation (16)

$$a^2 \sin\alpha = b^2 + (R^2 - b^2)\sin\beta$$

and using (23) and (35)

$$a^2 \sin\alpha = \mu^2 R^2 + (1-\mu^2)R^2 \sin\beta = R^2 \cos^2\xi_1$$

therefore

$$a\sqrt{\sin\alpha} = R\cos\xi_1. \tag{38}$$

But

$$\frac{\sqrt{2}\, s_1}{a} = \frac{\sqrt{2}\, s_1 \sqrt{\sin\alpha}}{a\sqrt{\sin\alpha}} = \frac{\sqrt{2}\, s_1 \cos\theta_1}{R\cos\xi_1}$$

where

$$\cos\theta_1 = \sqrt{\sin\alpha} \tag{39}$$

and hence equation (30) can be written in the form

$$\left(\frac{\sqrt{2}\, s_1}{R\cos\xi_1}\right)\cos\theta_1 = F\left(\frac{\pi}{2}, \frac{1}{\sqrt{2}}\right) - F\left(\theta_1, \frac{1}{\sqrt{2}}\right).$$

Let

$$\lambda = \frac{\sqrt{2}\, s_1}{R\cos\xi_1} \tag{40}$$

then

$$\lambda = \left\{F\left(\frac{\pi}{2}, \frac{1}{\sqrt{2}}\right) - F\left(\theta_1, \frac{1}{\sqrt{2}}\right)\right\}\sec\theta_1. \tag{41}$$

Values of this function λ for $-\pi/2 \leqslant \theta_1 \leqslant \pi/2$ have been calculated and are given in Table 1 with the corresponding values of α.

At $\theta_1 = \pi/2$:

$$\lambda\left(\theta_1 = \frac{\pi}{2}\right) = \underset{\theta_1 \to \pi/2}{\mathrm{Lt}} \left\{ \frac{F\left(\frac{\pi}{2}, \frac{1}{\sqrt{2}}\right) - F\left(\theta_1, \frac{1}{\sqrt{2}}\right)}{\cos \theta_1} \right\}$$

and at $\theta_1 = \pi/2$ this is indeterminate. Applying L'Hôpital's rule:

$$\lambda\left(\theta_1 = \frac{\pi}{2}\right) = \underset{\theta_1 \to \pi/2}{\mathrm{Lt}} \left[\frac{\frac{d}{d\theta_1}\left\{ - F\left(\theta_1, \frac{1}{\sqrt{2}}\right)\right\}}{\frac{d}{d\theta_1}(\cos \theta_1)} \right]$$

$$= \underset{\theta_1 \to \pi/2}{\mathrm{Lt}} \left[\frac{1}{\sin \theta_1 \sqrt{(1 - \frac{1}{2} \sin^2 \theta_1)}} \right]$$

which is determinate at $\theta_1 = \pi/2$;
therefore

$$\lambda \to \sqrt{2}.$$

When $\theta_1 = -\pi/2$, λ is infinite and hence λ is restricted to lie in the range

$$\infty > \lambda > \sqrt{2}. \tag{42}$$

Thus for a possible equilibrium configuration λ must be greater than $\sqrt{2}$, and from (40) it follows that the inequality

$$\frac{s_1}{R} > \cos \xi_1 \tag{43}$$

must be satisfied.
But

$$\frac{s_1}{R} + \frac{s_2}{R} = \frac{L}{R}$$

and hence the following inequality must also be satisfied

$$\frac{s_2}{R} + \cos \xi_1 < \frac{L}{R}. \tag{44}$$

It is now a quite simple matter to determine whether a given system can have an equilibrium configuration, and conversely it is possible to predict systems which will have an equilibrium configuration and be capable of supporting a given load under a given pressure.

As an example of the assessment of a system suppose that R_1, R, b, s_1 and s_2 are given. It is firstly postulated that

$$0 < \mu = \frac{b}{R} < \frac{1}{\sqrt{2}}.$$

We calculate s_2/R and also

$$\sin \delta = \frac{R_1^2 - b^2}{R^2 - b^2}. \tag{45}$$

Now from (34)

$$\frac{s_2}{R} = \frac{\sqrt{(1-\mu^2)}}{\sqrt{2}} \left[F\left(\xi_1, \frac{1}{\sqrt{\{2(1-\mu^2)\}}}\right) - F\left(\xi_2, \frac{1}{\sqrt{\{2(1-\mu^2)\}}}\right)\right] \tag{46}$$

where

$$\xi_1 = \cos^{-1} \sqrt{\{(1-\mu^2)\sin\beta + \mu^2\}} \tag{47}$$

and

$$0 \leqslant \xi_1 \leqslant \frac{\pi}{2},$$

also

$$\xi_2 = \cos^{-1} \sqrt{\{(1-\mu^2)\sin\delta + \mu^2\}}. \tag{48}$$

From equation (45) there are two possible values for δ:

(i) such that $\delta \geqslant \pi/2$ when $0 \leqslant \xi_2 \leqslant \pi/2$ and

(ii) such that $\delta \leqslant \pi/2$ when $-\pi/2 \leqslant \xi_2 \leqslant 0$.

For $\delta \geqslant \pi/2$, s_2/R cannot be greater than the maximum possible arc length between the points where

$$\varphi = \sin^{-1}\left(-\frac{\mu^2}{1-\mu^2}\right) \quad \text{and} \quad \varphi = \frac{\pi}{2}:$$

hence the inequality

$$\frac{s_2}{R} < \frac{\sqrt{(1-\mu^2)}}{\sqrt{2}} F\left(\frac{\pi}{2}, \frac{1}{\sqrt{\{2(1-\mu^2)\}}}\right) \tag{49}$$

must be satisfied.

For $\delta \leqslant \pi/2$, s_2/R cannot be greater than the maximum arc length between

$$\varphi = \sin^{-1}\left(-\frac{\mu^2}{1-\mu^2}\right) \quad \text{and} \quad \varphi = \pi - \sin^{-1}\left(-\frac{\mu^2}{1-\mu^2}\right)$$

and hence

$$\frac{s_2}{R} < \sqrt{\{2(1-\mu^2)\}} F\left(\frac{\pi}{2}, \frac{1}{\sqrt{\{2(1-\mu^2)\}}}\right). \tag{50}$$

It should be noted that the inequalities (49) and (50) merely provide upper bounds and do not tell us whether $\delta \geqslant \pi/2$ or $\leqslant \pi/2$, unless the inequality (50) is satisfied and (49) not satisfied; in this case δ must be $\geqslant \pi/2$. If the inequality (49) is satisfied δ may lie in either region.

Let us suppose that the inequality (49) is satisfied without (50) being satisfied, or that both (49) and (50) are satisfied; it should then be possible to find the equilibrium configuration. Suppose it is assumed that $\delta \geqslant \pi/2$ with $0 \leqslant \xi_2 \leqslant \pi/2$.

We form

$$\frac{s_2}{R} + \frac{\sqrt{(1-\mu^2)}}{\sqrt{2}} F\left(\xi_2, \frac{1}{\sqrt{\{2(1-\mu^2)\}}}\right)$$

and using a set of tables of elliptic integrals we endeavour to find a value of ξ_1, such that $0 \leqslant \xi_1 \leqslant \pi/2$, which makes this expression equal to

$$\frac{\sqrt{(1-\mu^2)}}{\sqrt{2}} F\left(\xi_1, \frac{1}{\sqrt{\{2(1-\mu^2)\}}}\right).$$

If there is no value of ξ_1 satisfying this then $\delta < \pi/2$ and $-\pi/2 \leqslant \xi_2 < 0$. In this manner the value of δ is found and also the value of ξ_1. Equation (47) now enables β to be found and

$$\sin\beta = \frac{\cos^2\xi_1 - \mu^2}{1-\mu^2} \tag{51}$$

where

$$\sin^{-1}\left(-\frac{\mu^2}{1-\mu^2}\right) < \beta < \frac{\pi}{2}.$$

An equilibrium configuration then exists if

$$\frac{s_1}{R} > \cos\xi_1.$$

Since s_1 is given, λ can be calculated and the corresponding value of α found from Table 1. Equations (32) and (37) can then be used to find the vertical co-ordinates x for the system and the configuration can be plotted graphically.

As another example of the assessment of a system suppose that the total generator-cord length L, the base radii R_1 and b, and the maximum lower-canopy radius R are given. Again, for equilibrium, it is postulated that

$$0 < \frac{b}{R} < \frac{1}{\sqrt{2}}.$$

We calculate L/R and if this is such that

$$\frac{L}{R} > \sqrt{\{2(1-\mu^2)\}}\,F\left(\frac{\pi}{2}, \frac{1}{\sqrt{\{2(1-\mu^2)\}}}\right)$$

then an equilibrium configuration exists provided that

$$\frac{s_2}{R} < \sqrt{\{2(1-\mu^2)\}}\,F\left(\frac{\pi}{2}, \frac{1}{\sqrt{\{2(1-\mu^2)\}}}\right).$$

If

$$\frac{L}{R} < \sqrt{\{2(1-\mu^2)\}}\,F\left(\frac{\pi}{2}, \frac{1}{\sqrt{\{2(1-\mu^2)\}}}\right)$$

then s_2/R must be chosen so that

$$\frac{s_2}{R} + \cos\xi_1 < \frac{L}{R}$$

and since $0 \leqslant \xi_1 \leqslant \pi/2$ this can be done with the aid of a set of tables. Having chosen s_1 and s_2 to satisfy the equilibrium conditions we may proceed as before and determine the complete configuration of the system.

4.3. *Some Practical Considerations.*

It is necessary to remark that, although the analysis of Section 4.2 may indicate that the system has an equilibrium configuration, it does not follow that this configuration is of any practical use: it is essential for the suspension points to lie above the plane surface at the base level otherwise the load can never be raised, and these points must also be high enough to accommodate the load and still allow it to be raised above the level of the base. This statement may seem trivial and obvious but it imposes limits on the values which can be taken for μ which are more stringent than that of $0 < \mu < 1/\sqrt{2}$.

In Fig. 10 are plotted some members of the family of curves for the lower canopy where

$$\sin\varphi = \frac{r^2 - b^2}{R^2 - b^2} = \frac{\left(\frac{r}{R}\right)^2 - \mu^2}{1 - \mu^2}$$

and reference to these curves readily reveals some interesting features. The maximum height of the suspension points for the load above the plane surface where $\varphi = \pi$, $\delta = 0$ and $r/R = \mu$ occurs when they are situated at the upper points given by $\varphi = 0$, $r/R = \mu$. If full advantage has to be taken of the maximum height of the lower canopy then the base angle δ must be zero; if $\delta = \pi/2$ then only half of this maximum height is available. The maximum height H can be obtained using equation (37) with $\beta = 0$ and $\varphi = \pi$ and is given by

$$\frac{H}{R} = 2\sqrt{\{2(1-\mu^2)\}}\, E\left[\cos^{-1}\mu, \frac{1}{\sqrt{\{2(1-\mu^2)\}}}\right] - 2\sqrt{\left(\frac{1-\mu^2}{2}\right)}\, F\left[\cos^{-1}\mu, \frac{1}{\sqrt{\{2(1-\mu^2)\}}}\right]$$

with

$$0 < \cos^{-1}\mu < \frac{\pi}{2}.$$

Values of H/R have been calculated for μ up to $0{\cdot}7$ and are given approximately in the Table below.

TABLE

Values of H/R for $0{\cdot}1 \leqslant \mu \leqslant 0{\cdot}7$

$\mu = \frac{b}{R}$	$\doteq \frac{H}{R}\ (\delta = 0)$
0·1	1·19
0·2	1·14
0·3	1·05
0·4	0·96
0·5	0·83
0·6	0·70
0·7	0·54

[The values given are only approximate: the reason for this is that the elliptic-functions tables of $E(\theta, k)$ and $F(\theta, k)$ are usually given with $\sin^{-1} k$ at intervals of 1° and θ at intervals of 5°. In order to obtain accurate values at intermediate points extensive interpolation is necessary, and in the circumstances not worthwhile, for the figures given should be accurate to about $\pm 2\%$ which for all practical purposes is adequate.]

If the system is to be efficient in the sense that the heaviest possible load can be lifted with the minimum pressure difference then μ should be fairly large, say $0{\cdot}6$ to $0{\cdot}7$. A disadvantage occurring here is that when μ is of this magnitude then H/R is rather small (about $0{\cdot}6$) and the lower canopy is rather squat; a large upper canopy may thus be required to accommodate the load. If the load is rather bulky and a tall lower canopy is required then the efficiency must be reduced and a higher pressure difference applied to raise the load. The upper canopy must in any case be such that the

load suspension points lie above the base level $\delta = 0$, $\varphi = \pi$ and in Fig. 10 the curve for $\mu = 0{\cdot}6960$ immediately shows that the radius of the circle at the suspension-point interface, r_1, must be such that r_1/R is greater than approximately $0{\cdot}1$; there is thus a minimum size for the interface radius r_1 whenever μ exceeds a certain value: this value can be determined by considering the case where there is no upper canopy. The first acceptable configuration (which is practically useless) is that where the single suspension point is on the same level as the base $\delta = 0$, $\varphi = \pi$. By plotting the difference between the maximum height ratio H/R and the distance between the suspension point where

$$\varphi = \sin^{-1}\left(-\frac{\mu^2}{1-\mu^2}\right)$$

and its image point where

$$\varphi = \pi - \sin^{-1}\left(-\frac{\mu^2}{1-\mu^2}\right)$$

(again as a ratio of distance/R), against μ, the value of μ for which this difference is unity can be obtained and gives the critical value for μ as being approximately $0{\cdot}665$. Hence, whenever μ exceeds $0{\cdot}665$ there must be an upper canopy and by plotting the curve for the required value of μ the minimum value for r_1 can be determined. Also, in order to make a system without an upper canopy and with a single suspension point it is essential that μ should be less than $0{\cdot}665$.

These criteria for μ have been referred to the case where $\delta = 0$ and if the system is designed with δ other than zero, say lying between 0 and $\pi/2$, the critical value for μ at which the suspension points are level with the base is further reduced and must be determined for each individual case by reference to the curve of

$$\sin\varphi = \frac{\left(\frac{r}{R}\right)^2 - \mu^2}{1-\mu^2}$$

for the appropriate value of μ. For $\delta = \pi/2$ the critical value is approximately $\mu = 0{\cdot}6$.

Practically, in order to keep the weight of the system and the amount of material used to a minimum it should be designed with the annular base of the same outer radius as the maximum radius of the lower canopy. The angle δ is then $\pi/2$ and there is no radial tension in the base hoop. However, if a wire grommet or tension cord is used for the base, $R_1 = b$, and then $\delta = 0$. A certain amount of extra fabric is required below the point B and the base cord may have to be substantial to withstand the radial tension loads. A possible shape is shown in Fig. 5.

If, on the other hand, δ is larger than $\pi/2$, the lower canopy does not attain the maximum radius R and there is a radial compression on the base. With the system envisaged the whole device is intended to be collapsible and the rigidity of the base obtained by means of inflated ribs; these may be satisfactory under tension but are liable to buckle under fairly low compression and it would appear undesirable to have a system designed with $\delta > \pi/2$.

In general, the most efficient and economical structure should be that designed with $\delta = \pi/2$ so that the radial stress in the base is zero. In this case the height of the system can be kept to a minimum, the centre of gravity as low as possible, and the base area to a maximum. These factors should all be instrumental in promoting the static and dynamic stability of the device. With a small base area and $\delta < \pi/2$ the system might easily be unstable when subjected to small disturbances.

It may be desirable for the generator cords in both the upper and lower canopies to be equally stressed. In this case

$$T_1 = T_2 \tag{52}$$

and from equations (2) and (5)

$$a^2 = R^2 - b^2, \tag{53}$$

also from equations (3) and (4)

$$\sin \alpha - \sin \beta = \frac{b^2}{a^2}. \tag{54}$$

These equations may be used for rapid calculation of a and α when β is known.

This section has been concerned with determining the configuration taken up by the generator cords of a system with specified geometric parameters, alternatively the equations derived enable one to design a system. Having determined the configuration of the generator cords it is necessary to consider a possible shape for the fabric gore lying between them, and to calculate the stress in this fabric.

5. *The Calculation of the Gore Shape.*

In choosing gore shapes for the canopies it is essential that these should be such that the initial assumption of zero generator stress in the fabric is satisfied as far as possible. Without crinkling the gore surface is not plane and as it is usual to cut the gore from a plane sheet of fabric and not to mould it, the true gore shape cannot be represented in two-dimensional co-ordinates. In order to avoid this difficulty and arrive at a gore shape which can be represented two-dimensionally and thus cut from a plane sheet, the method used is to specify a means of generating the true gore surface without crinkling, calculate the true gore length as measured along the mid-gore line and then to assume that the width of the gore to be cut from plane fabric is equal to the length of the arc of the gore generating curve lying between two adjacent generator cords. It is then demonstrated that the plane gore so derived must be gathered along the generator cords in order to make it fit and in consequence the fabric should make no appreciable contribution to the tension already existing in the generator cords. It should be emphasised that the plane gore shape derived in this report is merely a particular case and there are many possible alternatives depending on the shape of the gore generating curve.

Consider the plane MPQ (π_1) containing the normals to a pair of adjacent generator cords at corresponding points P and Q situated at equidistant intervals from the vertex O of the upper canopy. It is supposed that the surface of the gore of both the upper and lower canopies is generated by a circle of constant radius h, lying in the plane π_1, and passing through P and Q, sweeping down the generator cords from O to the base of the upper canopy and from there to the base hoop.

Let OD and OE be adjacent generator cords; P and Q corresponding points on these cords at distance r from the axis Ox; and M a point on Ox such that MP and MQ are the normals to OD and OE at P and Q respectively, as in Fig. 6. PHQ is an arc of the generating circle lying in the plane MPQ (π_1), this circle is centred at I and has a constant radius h; H is the mid-point of the arc PQ. Another circle, centred at M, and of radius

$$\text{PM} = r \operatorname{cosec} \psi,$$

lying in the plane π_1. cuts the line MIH at G and the arc PG (= GQ) subtends an angle ϵ at M as shown in Fig. 7. The arc HQ subtends an angle η at I. Now the straight line PQ $= 2r \sin \pi/n$ and hence

$$\epsilon = \sin^{-1}\left(\sin\frac{\pi}{n}\sin\psi\right). \tag{55}$$

From ΔIQM:

$$\frac{h}{\sin\frac{\pi}{n}\sin\psi} = \frac{r\ \mathrm{cosec}\ \psi}{\sin(\pi-\eta)} = \frac{r\ \mathrm{cosec}\ \psi}{\sin\eta}$$

therefore

$$\sin\eta = \frac{r}{h}\sin\frac{\pi}{n}. \tag{56}$$

Let arc HQ $= w = h\eta$
then

$$w = h\sin^{-1}\left(\frac{r}{h}\sin\frac{\pi}{n}\right) \tag{57}$$

and this equation gives a measure of the half-gore width.

To obtain the length of the gore consider Fig. 8. Let

$$\mathrm{PP'} = \mathrm{QQ'} = \delta s \tag{58}$$

$$\mathrm{HH'} = dS \tag{59}$$

where s is arc length measured along the generator cord and S arc length measured along the mid-gore line.

Now

$$ds \doteqdot \mathrm{M_1G}\delta\psi$$

$$\mathrm{M_1H}\delta\psi \doteqdot \mathrm{HH'}$$

$$\mathrm{M_1H} = \mathrm{M_1G} + \mathrm{GH}$$

therefore

$$\frac{dS}{ds} = \operatorname*{Lt}_{\mathrm{P}\to\mathrm{P'}}\frac{\mathrm{HH'}}{\mathrm{PP'}} = \mathrm{Lt}\left(\frac{\mathrm{M_1G}+\mathrm{GH}}{\mathrm{M_1G}}\right)$$

$$\doteqdot 1 + \mathrm{GH}\frac{d\psi}{ds} \tag{60}$$

$$\mathrm{GH} = \mathrm{MI} + \mathrm{IH} - \mathrm{MG}$$

$$= \mathrm{MI} + h - r\ \mathrm{cosec}\ \psi.$$

But, from ΔIQM,

$$\frac{\mathrm{MI}}{\sin\mathrm{IQM}} = \frac{r\ \mathrm{cosec}\ \psi}{\sin\eta}$$

and

$$\mathrm{IQM} = \eta - \sin^{-1}\left(\sin\frac{\pi}{n}\sin\psi\right)$$

therefore

$$\mathrm{GH} = r\ \mathrm{cosec}\ \psi\sqrt{\left(1-\sin^2\frac{\pi}{n}\sin^2\psi\right)} - r\sin\frac{\pi}{n}\cot\eta + h - r\ \mathrm{cosec}\ \psi$$

and using (56)

$$\mathrm{GH} = r\ \mathrm{cosec}\ \psi\sqrt{\left(1-\sin^2\frac{\pi}{n}\sin^2\psi\right)} - h\sqrt{\left(1-\frac{r^2}{h^2}\sin^2\frac{\pi}{n}\right)} + h - r\ \mathrm{cosec}\ \psi.$$

Hence, to first-order terms:

$$\mathrm{GH} = \frac{1}{2} r \sin^2 \frac{\pi}{n} \left[\frac{r}{h} - \sin \psi \right]. \tag{61}$$

From (60) and (61):

$$\frac{dS}{ds} = 1 + \frac{1}{2} r \sin^2 \frac{\pi}{n} \left[\frac{r}{h} - \sin \psi \right] \frac{d\psi}{ds}. \tag{62}$$

[This form, and the preceding analysis of the gore shape, is almost identical with that used in the calculation of the gore shape for a parachute with cords over the canopy (*see* Ref. 1), but in the present case n is not assumed to be large and the exact value for the angle ϵ is used, as opposed to an approximate value.]

5.1. *The Upper-Canopy Gore.*

For the upper canopy:

$$\sin \psi = \frac{r^2}{a^2} \quad \text{and} \quad \frac{d\psi}{ds} = \frac{2r}{a^2}.$$

Substituting in equation (62)

$$\frac{S-s}{a} = \sin^2 \frac{\pi}{n} \int_0^{r/a} \left\{ \frac{a}{h} \left(\frac{r}{a} \right)^3 - \left(\frac{r}{a} \right)^4 \right\} \frac{d\left(\frac{r}{a} \right)}{\sqrt{\left\{ 1 - \left(\frac{r}{a} \right)^4 \right\}}}. \tag{63}$$

Performing the integration:

$$\frac{S-s}{a} = \sin^2 \frac{\pi}{n} \left[\frac{a}{2h} \left\{ 1 - \left(1 - \frac{2rh}{3a^2} \right) \sqrt{\left(1 - \left(\frac{r}{a} \right)^4 \right)} \right\} \right] +$$

$$+ \frac{1}{3\sqrt{2}} \sin^2 \frac{\pi}{n} \left[F\left(\cos^{-1} \frac{r}{a}, \frac{1}{\sqrt{2}} \right) - F\left(\frac{\pi}{2}, \frac{1}{\sqrt{2}} \right) \right] \tag{64}$$

and also from (30)

$$\frac{s}{a} = \frac{1}{\sqrt{2}} \left\{ F\left(\frac{\pi}{2}, \frac{1}{\sqrt{2}} \right) - F\left(\cos^{-1} \frac{r}{a}, \frac{1}{\sqrt{2}} \right) \right. . \tag{65}$$

Hence, given the values for n and h, equations (57), (64) and (65) can be used to determine the gore shape for the upper canopy.

5.2. *The Lower-Canopy Gore.*

For the lower canopy:

$$\sin \varphi = \frac{r^2 - b^2}{R^2 - b^2} \quad \text{and} \quad \frac{d\varphi}{ds} = \frac{2r}{R^2 - b^2}.$$

Putting $b = \mu R$ and substituting in (62)

$$\frac{S-s}{R} = \frac{\sin^2 \frac{\pi}{n}}{(1-\mu^2)} \int_{r_1/R}^{r/R} \frac{\left\{ \mu^2 + \frac{R}{h}(1-\mu^2) \frac{r}{R} - \left(\frac{r}{R} \right)^2 \right\} \left(\frac{r}{R} \right)^2}{\sqrt{\left[\left\{ 1 - \left(\frac{r}{R} \right)^2 \right\} \left\{ (1-2\mu^2) + \left(\frac{r}{R} \right)^2 \right\} \right]}} d\left(\frac{r}{R} \right). \tag{66}$$

The evaluation of this integral is described in Appendix I and the result is:

$$\frac{S-s}{R} = \sin^2\frac{\pi}{n}\left[\frac{\sqrt{2}\,\mu^2}{3\sqrt{(1-\mu^2)}}\,E\left(\cos^{-1}\frac{r}{R}, \frac{1}{\sqrt{\{2(1-\mu^2)\}}}\right) + \right.$$

$$+ \frac{\sqrt{2}\,(1-2\mu^2)}{6\sqrt{(1-\mu^2)}}\,F\left(\cos^{-1}\frac{r}{R}, \frac{1}{\sqrt{\{2(1-\mu^2)\}}}\right) +$$

$$+ \left(\frac{1}{3(1-\mu^2)}\frac{r}{R} - \frac{R}{2h}\right)\sqrt{\left[\left\{1-\left(\frac{r}{R}\right)^2\right\}\left\{(1-2\mu^2)+\left(\frac{r}{R}\right)^2\right\}\right]} -$$

$$\left. - \frac{\mu^2 R}{h}\sin^{-1}\sqrt{\frac{1-\left(\frac{r}{R}\right)^2}{2(1-\mu^2)}}\right]_{r_1/R}^{r/R} \tag{67}$$

also from equation (34)

$$\frac{s}{R} = \frac{\sqrt{(1-\mu^2)}}{\sqrt{2}}\left[F\left(\cos^{-1}\frac{r_1}{R}, \frac{1}{\sqrt{\{2(1-\mu^2)\}}}\right) - F\left(\cos^{-1}\frac{r}{R}, \frac{1}{\sqrt{\{2(1-\mu^2)\}}}\right)\right]. \tag{68}$$

Equations (67) and (68), in conjunction with equation (57), enable the gore shape for the lower canopy to be determined and hence the shape of the gore for the whole canopy is known.

Suppose that the gore for the upper canopy is cut to the shape $OP_1H_1Q_1$ and that for the lower canopy to the shape $P_1P_2H_2Q_2Q_1$ as shown in Fig. 9. For the upper canopy S is measured downwards from O as far as H_1 and for the lower canopy it is measured from H_1 down to H_2 with w as the semi-gore width. The points P_1 and Q_1 are made to correspond to two adjacent suspension points on the generator cords and P_2 and Q_2 to two adjacent points on the base hoop.

Now

$$OP_1 > OH_1 > s_1,$$

where s_1 is the total length of the upper-canopy generator cord, and hence when the fabric OP_1 is ranged along this generator cord it must be slack in comparison with the cord itself. Similarly for the lower-canopy gore

$$P_1P_2 > H_1H_2 > s_2$$

and the fabric P_1P_2 when ranged along the generator cord is slack compared with the cord itself.

The particular type of gore generated by the circle of radius h thus satisfies the assumption made in Section 2 that the gore fabric should have a minimum of tension in the direction of the generator cord.

5.3. *Stresses in the Fabric Gore.*

If the extension of the fabric used for the gore is neglected the approximate circumferential tension can be calculated using membrane theory. It has been assumed that the generator tension in the gore fabric is negligibly small in comparison with the circumferential tension in this fabric; this implies that the radius of curvature of the gore fabric in the generator direction is very large

in comparison with that in the circumferential direction. In these circumstances the radius of curvature in the circumferential direction is approximately equal to the radius of the gore generating circle h and approximately

$$p = \frac{T_c}{h} \tag{69}$$

where T_c is the circumferential tension *in the fabric*. Using equation (7):

$$T_c = \frac{Mgh}{\pi b^2}. \tag{70}$$

If the yield strength of the fabric is $T_{c\max}$ then the maximum load which the system might be expected to support is given by

$$(Mg)_{\max} = \frac{\pi b^2}{h} T_{c\max} \tag{71}$$

which can be written

$$(Mg)_{\max} = \frac{\pi}{2} \frac{a}{h} \frac{b}{a} 2b T_{c\max}. \tag{72}$$

Thus, the greater the value of a/h or b/a the greater is the maximum load the system can support without the fabric breaking down.

The values of a/h (or R/h) determine the fullness of the gores and the larger these ratios the less the tension in the fabric for a given load, which enables a low-tensile-strength fabric to be used. The actual bulk of the fabric system is directly proportional to the area of a gore and the fabric thickness—the gore area increases with $1/h$ and the fabric stresses are reduced—so that the optimum value for h should occur when the product of the gore area and $1/h$ is a minimum. This minimum is of particular interest if the bulk of the system is of major importance: in parachute theory, which corresponds to the upper canopy only, it is usual to take a value for a/h of two (2) as this gives an approximate minimum, this is probably a reasonable value to take for the present system.

It must be stressed that the theory involved in the calculation of the gore shape is at best a very crude approximation. It may be better to design the gore so that the value of 'h' for the upper canopy is different to that for the lower canopy, e.g. for the upper canopy so that $a/h = 2$ and for the lower canopy so that $R/h = 2$, and it is then necessary to match the fabric shape at the suspension-point interface. It may be desirable to have very little fabric billowing between the generator cords, in this case a stronger fabric with a larger value for h may be required. These factors must be determined in relation to the requirements for a particular system and experiment will finally decide whether a system is satisfactory.

6. *Conclusions.*

The analysis shows that an equilibrium configuration can only exist for the model system allowing for single-point suspension if the base orifice area is less than half the total projected area of the lower canopy and that further restrictions of a geometric nature then determine whether an equilibrium configuration is possible; these latter restrictions can only affect such factors as the total height of the system and the position of the points of attachment of the load cords. All the necessary formulae for the design of the system are given, including the calculation of a particular

type of gore shape, and an estimate is also made of the maximum load which could be carried with a given fabric and system geometry. The tensions in the generator cords can be determined easily and an approximation is given for the tension in the gore fabric.

The advantage of the structure considered, apart from the fact that it lends itself to approximate analysis and provides a theoretical design basis which could readily be applied using nothing more than a set of tables and a hand calculating machine, is that it makes the most economical use of fabric, the approximate stress distribution is known, and full account can be taken of design requirements such as maximum permissible height or headroom, position of load and the total bulk of the structure. Practically there seems to be no serious difficulty involved in constructing a system of this type; care is needed in choosing fabrics and, although inextensibility is desirable to accord with the theory, as long as the extensibility of the generator cords is less than that of the fabric gore the theory should give a reasonable approximation.

LIST OF SYMBOLS

$E(\varphi, k)$		Legendre's incomplete elliptic integral of the second kind
$F(\varphi, k)$	=	u, incomplete elliptic integral of the first kind
F		Tension in a load cord
H		Maximum height of the lower canopy
L		Total generator-cord length from the apex to the base of the system
M		The load mass
R		Maximum radius of the lower canopy
R_1		Outer radius of the annular base hoop
S		The arc length for the fabric measured along the mid-gore line
T_1		Tension in the upper-canopy generator cord
T_2		Tension in the lower-canopy generator cord
T_3		Radial tension in a base hoop rib
T_c		Tension in the circumferential direction in the gore fabric
a		Maximum radius of the upper canopy
b		Radius of the orifice in the base hoop (a, b and c are also used in the Appendix in a different context in giving standard forms for elliptic integrals)
h		Radius of the gore-fabric generating circle
k		Modulus of the elliptic integrals
k'	=	$\sqrt{(1-k^2)}$, the complementary modulus
l		The length of a load cord
n		Number of generator and load cords
p		Pressure difference across the fabric
r		Radial distance
r_1		Radius at the canopy suspension-point interface
s		Arc length measured from various origins as stated in the text
s_1		Total arc length measured along a generator cord from the apex of the upper canopy to the suspension-point interface
s_2		Arc length measured along a generator cord of the lower canopy from the suspension-point interface to the base hoop
w		Semi-gore width of the fabric

LIST OF SYMBOLS—*continued*

x	Vertical distance measured from various origins as stated in the text
x_1	Height of the upper canopy from apex to suspension-point interface
x_2	Height of the lower canopy from the suspension-point interface to the base hoop
α	Angle made by the upper-canopy generator cord with the horizontal at the suspension-point interface
β	Angle made by the lower-canopy generator cord with the horizontal at the suspension-point interface
γ	Angle made by a load cord with the horizontal
δ	Angle made by a lower-canopy generator cord at the point of contact of the base hoop with a plane surface. (These angles α, β, γ, δ are measured in the directions shown in the figures)
ϵ	Angle defined in Section 5, equation (55)
η	Angle defined in Section 5
θ	Defined by equation (31) $= \cos^{-1}(\sqrt{\sin \psi})$
λ	Defined by equation (40) $= \dfrac{\sqrt{2}\, s_1}{R \cos \xi_1}$
μ	Parameter defined as $= \dfrac{b}{R}$
ξ, ξ_1	Defined in equations (35) and (36)
φ	Angle made by the tangent to the lower-canopy generator cords measured from the horizontal position $r = b$
ψ	Angle made by the tangent to the upper-canopy generator cords measured from the horizontal position at the apex $r = 0$

REFERENCES

No.	*Author(s)*	*Title, etc.*
1	G. W. H. Stevens and T. F. Johns ..	The theory of parachutes with cords over the canopy. A.R.C. R. & M. 2320. July, 1942.
2	Jahnke-Emde-Lösch	*Tables of higher functions.* 6th edition, McGraw Hill Book Co. 1960.
3	P. F. Byrd and M. D. Friedman ..	*Handbook of elliptic integrals for engineers and physicists.* Springer-Verlag, Berlin. 1954.

TABLE 1

Values of λ *and* α *for* $-\pi/2 \leqslant \theta_1 \leqslant \pi/2$

$\lambda = \frac{\sqrt{2}\, s_1}{R \cos \xi}$	$\theta_1{}^\circ$	α°	$\lambda = \frac{\sqrt{2}\, s_1}{R \cos \xi}$	$\theta_1{}^\circ$	α°
∞	−90	0	1·8541	0	90°
104·8	−88	0° 4′	1·8203	2	92° 48′
51·76	−86	0° 17′	1·7885	4	95° 36′
34·07	−84	0° 37′	1·7589	6	98° 30′
25·23	−82	1° 7′	1·7311	8	101° 17′
19·941	−80	1° 43′	1·7051	10	104° 11′
16·421	−78	2° 28′	1·6805	12	106° 55′
13·913	−76	3° 21′	1·6577	14	109° 42′
12·038	−74	4° 21′	1·6364	16	112° 27′
10·585	−72	5° 29′	1·6166	18	115° 14′
9·426	−70	6° 43′	1·5979	20	117° 59′
8·482	−68	8° 4′	1·5804	22	120° 43′
7·699	−66	9° 31′	1·5643	24	123° 26′
7·040	−64	11° 5′	1·5493	26	126° 8′
6·477	−62	12° 44′	1·5354	28	128° 47′
5·993	−60	14° 29′	1·5225	30	131° 25′
5·5719	−58	16° 18′	1·5105	32	134° 1′
5·2027	−56	18° 13′	1·4995	34	136° 36′
4·8768	−54	20° 13′	1·4895	36	139° 7′
4·5873	−52	22° 17′	1·4802	38	141° 37′
4·3286	−50	24° 24′	1·4717	40	144° 4′
4·0966	−48	26° 36′	1·4640	42	146° 29′
3·8874	−46	28° 51′	1·4572	44	148° 50′
3·6980	−44	31° 10′	1·4509	46	151° 9′
3·5257	−42	33° 31′	1·4453	48	153° 24′
3·3690	−40	35° 56′	1·4403	50	155° 36′
3·2255	−38	38° 23′	1·4359	52	157° 43′
3·0942	−36	40° 53′	1·4319	54	159° 47′
2·9733	−34	43° 24′	1·4287	56	161° 47′
2·8621	−32	45° 59′	1·4259	58	163° 42′
2·7594	−30	48° 35′	1·4234	60	165° 31′
2·6646	−28	51° 13′	1·4214	62	167° 16′
2·5764	−26	53° 52′	1·4196	64	168° 55′
2·4947	−24	56° 34′	1·4181	66	170° 29′
2·4189	−22	59° 17′	1·4172	68	171° 56′
2·3484	−20	62° 1′	1·4163	70	173° 17′
2·2826	−18	64° 46′	1·4155	72	174° 31′
2·2212	−16	67° 33′	1·4152	74	175° 39′
2·1640	−14	70° 18′	1·4149	76	176° 39′
2·1103	−12	73° 5′	1·4147	78	177° 32′
2·0603	−10	75° 49′	1·4146	80	178° 17′
2·0135	− 8	78° 43′	1·4145	82	178° 53′
1·9697	− 6	81° 30′	1·4144	84	179° 23′
1·9286	− 4	84° 24′	1·4143	86	179° 43′
1·8901	− 2	87° 12′	1·4142	88	179° 56′
1·8541	0	90°	1·4142	90	180°

APPENDIX I

Evaluation of the Elliptic Integrals

The integrals of Section 4 are of the type:

$$I_1 = \frac{1}{2}\int \frac{d\psi}{\sqrt{\sin\psi}}; \qquad I_2 = \frac{1}{2}\int \sqrt{\sin\psi}\, d\psi;$$

$$I_3 = \frac{1}{2}\int \frac{(1-\mu^2)d\psi}{\sqrt{\{(1-\mu^2)\sin\psi + \mu^2\}}}; \qquad I_4 = \frac{1}{2}\int \frac{(1-\mu^2)\sin\psi d\psi}{\sqrt{\{(1-\mu^2)\sin\psi + \mu^2\}}};$$

where $2\mu^2 - 1 \leqslant 0$, and the integrals are taken between the appropriate limits. In I_1 and I_2 set $\sin\psi = t^2$ and in I_3 and I_4 set $(1-\mu^2)\sin\psi + \mu^2 = t^2$, whence on re-arranging in the appropriate form:

$$I_1 = \int \frac{dt}{\sqrt{\{(1-t^2)(1+t^2)\}}};$$

$$I_2 = \int \frac{t^2 dt}{\sqrt{\{(1-t^2)(1+t^2)\}}} = \int \sqrt{\left(\frac{1+t^2}{1-t^2}\right)}\, dt - I_1;$$

$$I_3 = \int \frac{(1-\mu^2)dt}{\sqrt{\{(1-t^2)(1-2\mu^2+t^2)\}}}$$

and

$$I_4 = \int \frac{(t^2-\mu^2)dt}{\sqrt{\{(1-t^2)(1-2\mu^2+t^2)\}}} = \int \sqrt{\left(\frac{1-2\mu^2+t^2}{1-t^2}\right)}\, dt - I_3$$

taken between the appropriate limits. These integrals, in terms of t, may now be evaluated by making use of the following standard forms—(*see*, e.g. Ref. 2):
with

$$a^2 + b^2 = c^2,\ k = \frac{a}{c}$$

and

$$\Delta(\varphi, k) = \sqrt{\{1 - k^2\sin^2\varphi\}},$$

(i) $$\int_x^a \frac{dt}{\sqrt{\{(a^2-t^2)(b^2+t^2)\}}} = \frac{1}{c}F(\varphi, k)$$

where $\cos\varphi = x/a$;

(ii) $$\int_x^a \sqrt{\left(\frac{b^2+t^2}{a^2-t^2}\right)}\, dt = cE(\varphi, k)$$

where $\cos\varphi = x/a$;

(iii) $$\int_x^c \frac{dt}{\sqrt{\{(c^2-t^2)(t^2-b^2)\}}} = \frac{1}{c}F(\varphi, k)$$

where $\Delta(\varphi, k) = x/c$;

(iv) $$\int_x^c \frac{t^2 dt}{\sqrt{\{(c^2-t^2)(t^2-b^2)\}}} = cE(\varphi, k)$$

where $\Delta(\varphi, k) = x/c$.

$F(\varphi, k)$ is the Legendre normal integral of the first kind

$$F(\varphi, k) = \int_0^{\varphi} \frac{d\psi}{\sqrt{(1-k^2 \sin^2 \psi)}}$$

and $E(\varphi, k)$ is the normal integral of the second kind

$$E(\varphi, k) = \int_0^{\varphi} \sqrt{(1-k^2 \sin^2 \psi)} d\psi .$$

E and F are tabulated in most sets of tables of higher functions, usually in terms of φ and α where

$$E(\varphi, k) = E(\varphi, \sin \alpha)$$
$$F(\varphi, k) = F(\varphi, \sin \alpha)$$

such that

$$0 \leqslant \varphi \leqslant \frac{\pi}{2}, 0 \leqslant \alpha \leqslant \frac{\pi}{2}.$$

To extend the range of these tables one can make use of the following relations:

$$E(-\varphi, k) = -E(\varphi, k)$$
$$F(-\varphi, k) = -F(\varphi, k)$$
$$E(m\pi \pm \varphi, k) = 2mE\left(\frac{\pi}{2}, k\right) \pm E(\varphi, k)$$
$$F(m\pi \pm \varphi, k) = 2mF\left(\frac{\pi}{2}, k\right) \pm F(\varphi, k)$$

On evaluation the results obtained are:

$$I_1 = \frac{s}{a} = \frac{1}{2} \int_0^{\psi} \frac{d\psi}{\sqrt{\sin \psi}} = \frac{1}{\sqrt{2}} F\left(\frac{\pi}{2}, \frac{1}{\sqrt{2}}\right) - \frac{1}{\sqrt{2}} F\left(\theta, \frac{1}{\sqrt{2}}\right)$$

where

$$\theta = \cos^{-1}(\sqrt{\sin \psi});$$

$$I_2 = \frac{x}{a} = \frac{1}{2} \int_0^{\psi} \sqrt{\sin \psi} d\psi = \sqrt{2}\, E\left(\frac{\pi}{2}, \frac{1}{\sqrt{2}}\right) - \sqrt{2}\, E\left(\theta, \frac{1}{\sqrt{2}}\right) - I_1,$$

and the corresponding ranges for ψ and θ are discussed in the main text;

$$I_3 = \frac{s}{R} = \frac{1}{2} \int_{\beta}^{\varphi} \frac{(1-\mu^2) d\psi}{\sqrt{\{(1-\mu^2) \sin \psi + \mu^2\}}}$$
$$= \frac{\sqrt{(1-\mu^2)}}{\sqrt{2}} \left[F\left(\xi_1, \frac{1}{\sqrt{\{2(1-\mu^2)\}}}\right) - F\left(\xi, \frac{1}{\sqrt{\{2(1-\mu^2)\}}}\right) \right]$$

where

$$\xi_1 = \cos^{-1} \sqrt{\{(1-\mu^2) \sin \beta + \mu^2\}}$$

and

$$\xi = \cos^{-1} \sqrt{\{(1-\mu^2) \sin \varphi + \mu^2\}};$$

$$I_4 = \frac{x}{R} = \frac{1}{2} \int_{\beta}^{\varphi} \frac{(1-\mu^2) \sin \psi d\psi}{\sqrt{\{(1-\mu^2) \sin \psi + \mu^2\}}}$$
$$= \sqrt{\{2(1-\mu^2)\}} \left[E\left(\xi_1, \frac{1}{\sqrt{\{2(1-\mu^2)\}}}\right) - E\left(\xi, \frac{1}{\sqrt{\{2(1-\mu^2)\}}}\right) \right] - I_3,$$

the corresponding ranges for ξ and φ being discussed in the main text.

The integral (63) of Section 5.1 can be evaluated partly in terms of elementary functions and completed using the standard form (i). The integral (66) of Section 5.2 is slightly more complicated and can be written in the form

$$\frac{S-s}{R} = \frac{\mu^2 \sin^2 \frac{\pi}{n}}{\sqrt{2}(1-\mu^2)^{3/2}} \int_{t_0}^{t_1} \frac{t^2 dt}{\sqrt{\{(1-t^2)(k'^2+k^2t^2)\}}} +$$

$$+ \frac{R \sin^2 \frac{\pi}{n}}{\sqrt{2}(1-\mu^2)^{1/2}h} \int_{t_0}^{t_1} \frac{t^3 dt}{\sqrt{\{(1-t^2)(k'^2+k^2t^2)\}}} -$$

$$- \frac{\sin^2 \frac{\pi}{n}}{\sqrt{2}(1-\mu^2)^{3/2}} \int_{t_0}^{t_1} \frac{t^4 dt}{\sqrt{\{(1-t^2)(k'^2+k^2t^2)\}}}$$

where

$$k^2 = 1 - k'^2 = \frac{1}{2(1-\mu^2)}; \; t = \frac{r}{R}.$$

These three integrals can be evaluated using the following standard results: (*see* Ref. 3)

$$C_m = -\int \frac{t^m dt}{\sqrt{\{(1-t^2)(k'^2+k^2t^2)\}}} = \int \frac{\cos^m \varphi d\varphi}{\sqrt{(1-k^2 \sin^2 \varphi)}}$$

$$= \int \mathrm{cn}^m u du$$

where

$$t = \cos \varphi = \mathrm{cn}\, u.$$

$$C_0 = \int du = u = F(\varphi, k) \, (\varphi = \mathrm{am}\, u)$$

$$C_1 = \int \mathrm{cn}\, u du = \frac{\cos^{-1}(\mathrm{dn}\, u)}{k} = \frac{\sin^{-1}(k \,\mathrm{sn}\, u)}{k}$$

$$C_2 = \int \mathrm{cn}^2 u du = \frac{1}{k^2}[E(\varphi, k) - k'^2 u]$$

$$C_3 = \int \mathrm{cn}^3 u du = \frac{1}{2k^3}[(2k^2-1)\sin^{-1}(k \,\mathrm{sn}\, u) + k \,\mathrm{sn}\, u \,\mathrm{dn}\, u]$$

$$C_4 = \int \mathrm{cn}^4 u du$$

$$= \frac{1}{3k^4}[(2-3k^2)k'^2 u + 2(2k^2-1)E(\varphi, k) + k^2 \,\mathrm{sn}\, u \,\mathrm{cn}\, u \,\mathrm{dn}\, u]$$

where

$$\mathrm{sn}\,(u, k) = \sin \varphi$$

$$\mathrm{cn}\,(u, k) = \cos \varphi$$

$$\mathrm{dn}\,(u, k) = \sqrt{[1 - k^2 \sin^2 \{\mathrm{am}\,(u, k)\}]}$$

$$\varphi = \mathrm{am}\,(u, k); \; u = F(\varphi, k);$$

and the relations

$$\begin{aligned} \mathrm{sn}^2 u + \mathrm{cn}^2 u &= 1 \\ \mathrm{dn}^2 u &= 1 - k^2 \mathrm{sn}^2 u \\ &= k'^2 + k^2 \mathrm{cn}^2 u \\ &= \mathrm{cn}^2 u + k'^2 \mathrm{sn}^2 u \end{aligned}$$

enable the integrals to be reduced to more convenient forms.

The result of the integration is given as equation (67).

APPENDIX II

Tabulated Co-ordinates for the Canopy and Gore Shapes

The values of x/R and r/R are given in Table 1 for the following values of μ: 0·1833, 0·2555, 0·3074, 0·3845, 0·5050, 0·5773, 0·6585 and 0·6960. Using this table the lower-canopy shapes given by

$$\sin \varphi = \frac{\left(\frac{r}{R}\right)^2 - \mu^2}{1 - \mu^2}$$

can be plotted graphically: this is done in Fig. 10.

The co-ordinates in Table 2 for the upper-canopy shape are calculated using

$$\sin \psi = \frac{r^2}{a^2}$$

and give the Taylor shape.

Table 3 gives the gore co-ordinates for the upper canopy. This table is calculated with $a/h = 2{\cdot}0$; $n = 8$, 12 and 16. The semi-gore shape for $n = 8$ is plotted in Fig. 11 up to $r/a = 1{\cdot}0$. From the table it can be seen that the differences between the gore lengths for $n = 8$, 12 and 16 are only a few per cent and in practice these differences may be of little significance.

The gore co-ordinates for the lower canopy are given in Table 4. This table has been calculated for $R/h = 2{\cdot}0$; $n = 8$, 12 and 16; and for the same range of values of μ as in Table 1. The semi-gore shapes for $R/h = 2{\cdot}0$; $n = 8$; $\mu = 0{\cdot}5050$, 0·6585 and 0·6960 are shown plotted in Fig. 12. For values of μ below 0·5773 the gore shape is practically unchanged as is evident by referring to Table 4; only for higher values of μ do appreciable changes occur.

TABLE 1

The Lower-Canopy Co-ordinates

Values of $\frac{x}{R}$

$\frac{r}{R}$	$\mu =$ 0·1833	$\mu =$ 0·2555	$\mu =$ 0·3074	$\mu =$ 0·3845	$\mu =$ 0·5050	$\mu =$ 0·5773	$\mu =$ 0·6585	$\mu =$ 0·6960
0·000	0·000	0·000	0·000	0·000	0·000	0·000	0·000	0·000
0·087	−0·003	−0·006	−0·009	−0·015	−0·031	−0·050	−0·102	−0·230
0·174	−0·004	−0·010	−0·016	−0·028	−0·060	−0·096	−0·196	−0·416
0·259	−0·003	−0·012	−0·021	−0·039	−0·085	−0·137	−0·276	−0·553
0·342	+0·002	−0·010	−0·021	−0·044	−0·104	−0·169	−0·339	−0·652
0·423	0·012	−0·003	−0·017	−0·044	−0·116	−0·193	−0·387	−0·722
0·500	0·026	+0·010	−0·006	−0·038	−0·120	−0·207	−0·420	−0·770
0·574	0·046	0·028	+0·010	−0·026	−0·117	−0·212	−0·439	−0·801
0·643	0·072	0·052	0·032	−0·007	−0·106	−0·208	−0·447	−0·817
0·707	0·103	0·082	0·060	+0·018	−0·088	−0·196	−0·445	−0·820
0·766	0·140	0·117	0·094	0·049	−0·063	−0·176	−0·433	−0·813
0·819	0·182	0·157	0·133	0·085	−0·032	−0·150	−0·414	−0·798
0·866	0·228	0·202	0·176	0·126	+0·004	−0·118	−0·387	−0·775
0·906	0·278	0·251	0·224	0·172	0·045	−0·080	−0·355	−0·746
0·940	0·331	0·303	0·275	0·221	0·090	−0·039	−0·318	−0·712
0·966	0·387	0·358	0·329	0·273	0·139	+0·007	−0·278	−0·673
0·985	0·446	0·415	0·386	0·328	0·189	0·054	−0·234	−0·632
0·996	0·506	0·474	0·444	0·384	0·242	0·104	−0·189	−0·589
1·000	0·566	0·534	0·502	0·441	0·295	0·154	−0·143	−0·545
0·996	0·627	0·593	0·561	0·498	0·348	0·204	−0·096	−0·501
0·985	0·687	0·652	0·619	0·554	0·400	0·254	−0·051	−0·458
0·966	0·745	0·710	0·675	0·608	0·451	0·301	−0·007	−0·416
0·940	0·801	0·765	0·729	0·660	0·499	0·346	+0·033	−0·378
0·906	0·855	0·817	0·781	0·710	0·544	0·388	0·070	−0·344
0·866	0·905	0·866	0·828	0·755	0·585	0·425	0·102	−0·315
0·819	0·951	0·911	0·872	0·797	0·622	0·458	0·129	−0·292
0·766	0·993	0·951	0·911	0·833	0·652	0·484	0·148	−0·276
0·707	1·029	0·986	0·944	0·864	0·677	0·504	0·160	−0·270
0·643	1·060	1·016	0·972	0·889	0·695	0·516	0·162	−0·273
0·574	1·086	1·040	0·995	0·908	0·706	0·520	0·154	−0·289
0·500	1·106	1·058	1·011	0·920	0·709	0·515	0·135	−0·319
0·423	1·121	1·070	1·021	0·926	0·705	0·501	0·102	−0·368
0·342	1·131	1·077	1·026	0·926	0·693	0·477	+0·054	−0·438
0·259	1·135	1·080	1·025	0·920	0·674	0·444	−0·003	−0·537
0·176	1·137	1·078	1·021	0·910	0·650	0·404	−0·089	−0·674
0·087	1·135	1·074	1·014	0·897	0·621	0·358	−0·183	−0·860
0·000	1·132	1·068	1·004	0·881	0·589	0·308	−0·285	−1·090

TABLE 2

The Upper-Canopy Co-ordinates

$\frac{r}{a}$	$\frac{x}{a}$
0·000	0·000
0·087	0·000
0·174	0·000
0·259	0·006
0·342	0·013
0·423	0·025
0·500	0·042
0·574	0·064
0·643	0·092
0·707	0·125
0·766	0·163
0·819	0·206
0·866	0·254
0·906	0·305
0·940	0·360
0·966	0·417
0·985	0·476
0·996	0·537
1·000	0·598

TABLE 3

Gore Co-ordinates for the Upper Canopy

$\frac{r}{a}$	$\frac{S}{a}$			$\frac{w}{a}$		
	$n = 8$	$n = 12$	$n = 16$	$n = 8$	$n = 12$	$n = 16$
0·000	0·000	0·000	0·000	0·000	0·000	0·000
0·174	0·174	0·174	0·174	0·066	0·044	0·034
0·342	0·343	0·343	0·343	0·133	0·089	0·067
0·500	0·507	0·505	0·504	0·196	0·131	0·098
0·643	0·664	0·659	0·657	0·257	0·170	0·127
0·766	0·816	0·806	0·802	0·313	0·204	0·152
0·866	0·964	0·947	0·941	0·362	0·232	0·172
0·940	1·109	1·084	1·074	0·402	0·254	0·188
0·985	1·252	1·217	1·204	0·427	0·267	0·197
1·000	1·394	1·349	1·332	0·436	0·272	0·200

TABLE 4

Gore Co-ordinates for the Lower Canopy

$\frac{r}{R}$	$\frac{w}{R}$			$\frac{S}{R}$ $\mu = 0{\cdot}1833$			$\frac{S}{R}$ $\mu = 0{\cdot}2555$			$\frac{S}{R}$ $\mu = 0{\cdot}3074$			$\frac{S}{R}$ $\mu = 0{\cdot}3845$		
	$n = 8$	$n = 12$	$n = 16$	$n = 8$	$n = 12$	$n = 16$	$n = 8$	$n = 12$	$n = 16$	$n = 8$	$n = 12$	$n = 16$	$n = 8$	$n = 12$	$n = 16$
0·000	0·000	0·000	0·000	0·000	0·000	0·000	0·000	0·000	0·000	0·000	0·000	0·000	0·000	0·000	0·000
0·174	0·066	0·044	0·034	0·176	0·175	0·174	0·174	0·174	0·174	0·174	0·174	0·174	0·176	0·176	0·176
0·342	0·133	0·089	0·067	0·343	0·343	0·342	0·344	0·343	0·343	0·344	0·344	0·343	0·346	0·346	0·345
0·500	0·196	0·131	0·098	0·506	0·504	0·503	0·506	0·504	0·503	0·506	0·504	0·503	0·509	0·506	0·505
0·643	0·257	0·170	0·127	0·663	0·657	0·655	0·622	0·656	0·654	0·661	0·655	0·653	0·663	0·656	0·653
0·766	0·313	0·204	0·152	0·814	0·803	0·799	0·812	0·800	0·796	0·810	0·798	0·794	0·810	0·797	0·792
0·866	0·362	0·232	0·172	0·960	0·942	0·935	0·957	0·938	0·931	0·954	0·934	0·927	0·952	0·930	0·922
0·940	0·402	0·254	0·188	1·103	1·077	1·067	1·090	1·071	1·061	1·094	1·066	1·055	1·090	1·059	1·048
0·985	0·427	0·267	0·197	1·244	1·208	1·195	1·238	1·201	1·187	1·232	1·194	1·180	1·225	1·183	1·168
1·000	0·436	0·272	0·200	1·384	1·338	1·321	1·376	1·329	1·311	1·369	1·320	1·302	1·358	1·307	1·288

$\frac{r}{R}$	$\frac{S}{R}$ $\mu = 0{\cdot}5050$			$\frac{S}{R}$ $\mu = 0{\cdot}5773$			$\frac{S}{R}$ $\mu = 0{\cdot}6585$			$\frac{S}{R}$ $\mu = 0{\cdot}6960$		
	$n = 8$	$n = 12$	$n = 16$	$n = 8$	$n = 12$	$n = 16$	$n = 8$	$n = 12$	$n = 16$	$n = 8$	$n = 12$	$n = 16$
0·000	0·000	0·000	0·000	0·000	0·000	0·000	0·000	0·000	0·000	0·000	0·000	0·000
0·174	0·184	0·184	0·184	0·199	0·199	0·199	0·263	0·263	0·262	0·452	0·452	0·451
0·342	0·360	0·359	0·359	0·385	0·384	0·383	0·489	0·486	0·485	0·751	0·746	0·744
0·500	0·524	0·520	0·519	0·555	0·550	0·548	0·678	0·669	0·666	0·963	0·951	0·946
0·643	0·678	0·669	0·665	0·710	0·698	0·694	0·840	0·822	0·816	1·134	1·111	1·102
0·766	0·823	0·806	0·800	0·854	0·833	0·826	0·985	0·956	0·946	1·282	1·246	1·232
0·866	0·961	0·935	0·925	0·990	0·959	0·947	1·119	1·077	1·062	1·416	1·365	1·347
0·940	1·094	1·057	1·044	1·119	1·077	1·061	1·244	1·190	1·170	1·540	1·475	1·541
0·985	1·223	1·175	1·158	1·244	1·190	1·170	1·364	1·297	1·272	1·657	1·578	1·550
1·000	1·351	1·292	1·270	1·368	1·301	1·277	1·482	1·401	1·371	1·772	1·679	1·645

APPENDIX III

The Configuration of the System before the Equilibrium Position is Attained

Consider a lifting structure designed in accordance with the theory of the main text and only partially pressurised. The load is assumed to be clear of the ground but the extent of the pressurisation is such that the equilibrium configuration still has to be attained. During the inflation process the only constant factors are the arc lengths of the generator cords and the inner and outer radii of the base; before the design equilibrium configuration is taken up it is to be expected that at any instant of time the maximum radius R' of the lower canopy is somewhat larger than the design radius R, similarly the angle δ' differs from δ and so-on. Whilst the base is still in contact with the ground there must be a ground reaction, N say, acting upon it, and to analyse the series of configurations taken up by the structure before the equilibrium configuration is reached it is necessary to modify equations (4), (5) and (6) to take account of this ground reaction; hence, denoting by dashes the conditions at some time before reaching equilibrium:

$$p'\pi b^2 + N = Mg \tag{74}$$

$$p'\pi(R'^2 - b^2) = nT_2' + N \tag{75}$$

$$p'\pi(R_1^2 - b^2) = nT_2' \sin\delta' + N. \tag{76}$$

Setting

$$Mg = p'\pi C^2 \tag{77}$$

and proceeding as in Section 3.2 the equation of the lower-canopy generator cords is found to be

$$\sin\varphi' = \frac{r'^2 - C^2}{R'^2 - C^2} \tag{78}$$

or, with

$$C = \mu' R' \tag{79}$$

$$\sin\varphi = \left\{\frac{\left(\frac{r'}{R'}\right)^2 - \mu'^2}{1 - \mu'^2}\right\}. \tag{80}$$

In equation (80) $|\sin\varphi'| \leqslant 1$ and as in Section 4.1 the condition that

$$0 \leqslant \frac{1 - \left(\frac{r'}{R'}\right)^2}{1 - \mu'^2} \leqslant 2 \tag{81}$$

can be obtained. It follows from this that

$$0 < \mu' < 1$$

and also

$$2\mu'^2 - 1 \leqslant 0. \tag{82}$$

Hence

$$0 < C \leqslant \frac{R'}{\sqrt{2}}. \tag{83}$$

When the pressure p' is increased there is a resulting decrease in C from (77), since Mg is constant, and there is also a decrease in R'. The canopies continue to change shape during inflation until

$b = C$ and $R = R'$, at which stage the ground reaction is zero and the structure is about to leave the ground. Clearly, with a low pressure p' the value of C must be large, as must that for μ', and it is possible by assuming a constant generator-cord length to plot the changes in the canopy configuration with the variation of μ' from a high value at the start of inflation to the stage where the equilibrium configuration is reached and $\mu' = \mu$.

APPENDIX IV

A Higher Approximation to the Theory

Because of the particular type of construction, in which the fabric bows out between the canopy generator cords, the projected areas on which the pressure acts in equations (2) and (5) are underestimated and allowance should be made to account for this if a more accurate theory is required. Before it is possible to determine the true projected area the shape of the gore generating curve must be specified; in the particular case considered in this report it is assumed that, as in Section 5, the gore is generated by a circle of radius h.

For the upper canopy, referring to Fig. 7, the true maximum projected area can be obtained by putting

$$\psi = \frac{\pi}{2}; \text{PM} = \text{QM} = a = r \qquad \text{and} \qquad \epsilon = \frac{\pi}{n}:$$

it is $n\eta h^2 + 2n \times$ area ΔIQM and this is

$$nh^2 \sin^{-1}\left(\frac{a}{h}\sin\frac{\pi}{n}\right) + nah \sin\left[\sin^{-1}\left(\frac{a}{h}\sin\frac{\pi}{n}\right) - \frac{\pi}{n}\right].$$

It should be noted that when n is large this area is approximately

$$nh^2 \frac{a}{h}\frac{\pi}{n} + nah\left[\frac{a}{h}\frac{\pi}{n} - \frac{\pi}{n}\right] = \pi a^2$$

and the projected area πa^2 used in equation (2) is an adequate approximation. However, for a relatively small number of cords, such as might be used in a lifting structure, the approximation is not really accurate enough and it may be desirable to use the true projected area.

Hence, instead of equation (2), we may write

$$p\pi a_1^2 = nT_1 \tag{84}$$

where

$$\pi a_1^2 = nh^2 \sin^{-1}\left(\frac{a}{h}\sin\frac{\pi}{n}\right) + nah \sin\left[\sin^{-1}\left(\frac{a}{h}\sin\frac{\pi}{n}\right) - \frac{\pi}{n}\right]. \tag{85}$$

Proceeding as in Section 3.1 the equation of the upper-canopy generator cords is found to be

$$\left[\sin\psi\right]_{\psi_0}^{\psi} = \left[\frac{r^2}{a_1^2}\right]_{r_0}^{r}.$$

Now when $\psi = \pi/2$, $r = a$ and hence the cord equation is

$$\sin\psi = \frac{r^2 + a_1^2 - a^2}{a_1^2}. \tag{86}$$

At the canopy apex $r = 0$, but ψ cannot be zero unless $a = a_1$, consequently in general the canopy is not flat but slightly conical and

$$\sin\psi_0 = 1 - \frac{a^2}{a_1^2}. \tag{87}$$

At the actual apex there is a discontinuity in the slope of the cords; for example with $a/h = 2$ and $n = 8$ the angle ψ_0 is approximately 7°, and with $n = 12$ it is approximately 3°.

The vertical co-ordinate of the upper-canopy cords, measured downwards from the apex O, is given by

$$x = \int_{\sin^{-1}(1-a^2/a_1^2)}^{\psi} \frac{a_1^2 \sin\psi d\psi}{2\sqrt{\{a_1^2\sin\psi - (a_1^2 - a^2)\}}},$$

which on integration leads to

$$\frac{x}{a} = \sqrt{2}\,\frac{a_1}{a}\left[E\left(\frac{\pi}{2}, \frac{1}{\sqrt{2}}\,\frac{a}{a_1}\right) - E\left(\cos^{-1}\frac{r}{a}, \frac{1}{\sqrt{2}}\,\frac{a}{a_1}\right)\right] -$$

$$- \frac{1}{\sqrt{2}}\,\frac{a_1}{a}\left[F\left(\frac{\pi}{2}, \frac{1}{\sqrt{2}}\,\frac{a}{a_1}\right) - F\left(\cos^{-1}\frac{r}{a}, \frac{1}{\sqrt{2}}\,\frac{a}{a_1}\right)\right]. \tag{88}$$

Similarly for the lower canopy the true projected area is

$$nh^2 \sin^{-1}\left(\frac{R}{h}\sin\frac{\pi}{n}\right) + nRh\sin\left[\sin^{-1}\left(\frac{R}{h}\sin\frac{\pi}{n}\right) - \frac{\pi}{n}\right]$$

$$= \pi R'^2 \quad \text{say} \tag{89}$$

and equation (5) is replaced by

$$p\pi(R'^2 - b^2) = nT_2. \tag{90}$$

Proceeding as in Section 3.2

$$\left[\sin\varphi\right]_{\varphi_0}^{\varphi} = \left[\frac{r^2}{R'^2 - b^2}\right]_{r_0}^{r};$$

when

$$\varphi_0 = \beta; \quad r_0^2 = r_1^2 = a_1^2\sin\alpha - (a_1^2 - a^2)$$

and when

$$\varphi = \frac{\pi}{2}; \quad r = R,$$

hence the equation of the lower-canopy generator cords is

$$\sin\varphi = \frac{r^2 - (b^2 + R^2 - R'^2)}{R'^2 - b^2}. \tag{91}$$

The vertical co-ordinate for the lower cords, measured downwards from the suspension-point interface is given by

$$x = \int_{\beta}^{\varphi} \frac{(R'^2 - b^2)\sin\varphi d\varphi}{2\sqrt{\{(R'^2 - b^2)\sin\varphi + (b^2 + R^2 - R'^2)\}}},$$

which gives on integration, with $b = \mu R$,

$$\begin{aligned}\frac{x}{R} = \frac{R'}{R}\sqrt{\left[2\left\{1 - \left(\frac{R}{R'}\mu\right)^2\right\}\right]}\Bigg[E\left(\xi, \frac{1}{\sqrt{\left[2\left\{1 - \left(\frac{R}{R'}\mu\right)^2\right\}\right]}}\frac{R}{R'}\right) - \\ - E\left(\xi_1, \frac{1}{\sqrt{\left[2\left\{1 - \left(\frac{R}{R'}\mu\right)^2\right\}\right]}}\frac{R}{R'}\right)\Bigg] - \\ - \frac{R'}{R}\sqrt{\left\{\frac{1 - \left(\frac{R}{R'}\mu\right)^2}{2}\right\}}\Bigg[F\left(\xi, \frac{1}{\sqrt{\left[2\left\{1 - \left(\frac{R}{R'}\mu\right)^2\right\}\right]}}R'\right) - \\ - F\left(\xi_1, \frac{1}{\sqrt{\left[2\left\{1 - \left(\frac{R}{R'}\mu\right)^2\right\}\right]}}\frac{R}{R'}\right)\Bigg]\end{aligned} \tag{92}$$

where

$$\xi_1 = \cos^{-1}\sqrt{\left[\left\{1 - \left(\frac{R}{R'}\mu\right)^2\right\}\sin\beta + \frac{b^2 + R^2 - R'^2}{R'^2}\right]}$$

and

$$\xi = \cos^{-1}\sqrt{\left[\left\{1 - \left(\frac{R}{R'}\mu\right)^2\right\}\sin\varphi + \frac{b^2 + R^2 - R'^2}{R'^2}\right]}.$$

For a possible equilibrium configuration

$$|\sin\varphi| \leqslant 1$$

and using equation (91):

$$0 < \frac{R^2 - r^2}{R'^2 - b^2} \leqslant 2$$

or

$$r^2 \geqslant \left\{2\mu^2 + 1 - 2\left(\frac{R'}{R}\right)^2\right\} R^2$$

for all $r \leqslant R$ allowing for single-point suspension. This inequality can only be satisfied if

$$2\mu^2 + 1 - 2\left(\frac{R'}{R}\right)^2 \leqslant 0$$

or

$$0 < b \leqslant R\sqrt{\left\{\frac{2\left(\frac{R'}{R}\right)^2 - 1}{2}\right\}}. \tag{93}$$

Since $R'/R \geqslant 1$, μ can take somewhat larger values than the limiting value of $1/\sqrt{2}$ given in the main text; for example with $a/h = 2$ and $n = 8$, $R'/R \doteqdot 1{\cdot}075$ and for an equilibrium configuration

$$0 < \mu \leqslant 0{\cdot}81\,;$$

with $n = 12$, $R'/R \doteqdot 1{\cdot}031$ and for equilibrium $0 < \mu \leqslant 0{\cdot}75$.

Thus, for each particular case, given the values of n and a/h, it is possible to determine more exact equilibrium configurations than those given by the theory of the main text. However, it is difficult to assess the practical importance of the higher approximation to the theory: it is impossible to either cut or sew a fabric to the exact shape specified, the elasticity of the fabric has been neglected and the assumptions made initially are of a tentative nature; in consequence the first-order theory, which is simpler, should be acceptable and satisfactory for use in most cases. Should it prove necessary this more accurate theory can be developed on exactly the same lines as that given in the main text and calculations of the gore shape for a given system can be made.

In order to show the effect of having only a small number of cords, the co-ordinates of the upper canopy for the cases $n = 8$ and $n = 12$ with $a/h = 2{\cdot}0$ are given approximately in Table 1 and plotted in Fig. 13, together with the standard Taylor shape resulting from the first-order approximation, whose co-ordinates are given in Table 2 of Appendix II. It can be seen that with a small number of cords the upper canopy is not so flat as the Taylor shape and it is appreciably deeper. The upper canopy alone corresponds to the parachute with cords over the canopy, and it has been found in practice that parachutes designed according to the first approximation do take up a shape less flat and deeper than that predicted by the theory. There may thus be some justification for making use of the higher approximation when the number of cords is small.

TABLE 1

Higher-Approximation Co-ordinates for the Upper Canopy

$\frac{r}{a}$	$\frac{x}{a}$ $n = 8$	$\frac{x}{a}$ $n = 12$
0·000	0·000	0·000
0·174	0·026	0·014
0·342	0·060	0·036
0·500	0·108	0·074
0·643	0·174	0·132
0·766	0·259	0·209
0·866	0·361	0·304
0·940	0·476	0·414
0·985	0·602	0·534
1·000	0·733	0·660

APPENDIX V

The Configuration of the System with $\mu > 1/\sqrt{2}$

It has been shown in Section 4.1 that single-point suspension is impossible unless $\mu < 1/\sqrt{2}$ and that when $\mu > 1/\sqrt{2}$ an upper canopy is necessary and the radius of the suspension-point interface must satisfy the inequality

$$\left(\frac{r_1}{R}\right)^2 \geqslant 2\mu^2 - 1. \tag{94}$$

(This is a necessary but not sufficient condition.)

The integrals (24) and (25) of Section 4 for the arc length s and vertical co-ordinate x lead to different general results according to whether

$$2\mu^2 - 1 \lesseqgtr 0:$$

for the case where this expression is positive the integrals can be evaluated using the standard forms (iii) and (iv) of Appendix I to give

$$\frac{s}{R} = (1-\mu^2)\left[F\{\zeta_1, \sqrt{[2(1-\mu^2)]}\} - F\{\zeta, \sqrt{[2(1-\mu^2]}\}\right] \tag{95}$$

and

$$\frac{x}{R} = E\{\zeta_1, \sqrt{[2(1-\mu^2)]}\} - E\{\zeta, \sqrt{[2(1-\mu^2)]}\} -$$

$$- \mu^2\left[F\{\zeta_1, \sqrt{[2(1-\mu^2)]}\} - F\{\zeta, \sqrt{[2(1-\mu^2)]}\}\right] \tag{96}$$

where

$$\zeta_1 = \cos^{-1}\sqrt{\frac{1+\sin\beta}{2}} \tag{97}$$

$$\zeta = \cos^{-1}\sqrt{\frac{1+\sin\varphi}{2}}. \tag{98}$$

For $-\pi/2 \leqslant \varphi \leqslant \pi/2$: $\pi/2 \geqslant \zeta \geqslant 0$ where $\zeta = 0$ corresponds to $\varphi = \pi/2$ and $\zeta = \pi/2$ corresponds to $\varphi = -\pi/2$; for $\varphi \geqslant \pi/2$: $0 \geqslant \zeta \geqslant -\pi/2$ where $\zeta = 0$ corresponds to $\varphi = \pi/2$ and $\zeta = -\pi/2$ corresponds to $\varphi = 3\pi/2$.

It should be noted that when $\mu = 1/\sqrt{2}$ the equations (95) and (96) are identical with (34) and (37) respectively of Section 4.2, as is to be expected.

Using (96) in conjunction with the equation

$$\sin\varphi = \frac{\left(\frac{r}{R}\right)^2 - \mu^2}{1-\mu^2} \tag{99}$$

it is possible to plot the lower-canopy generator-cord shape for cases where $\mu > 1/\sqrt{2}$. As an example the case $\mu = 0{\cdot}7906$ ($\mu^2 = 0{\cdot}625$) has been plotted in Fig. 14, the origin has been arbitrarily placed on the x/R axis so that $x/R = 0$ coincides with $\varphi = -\pi/2$ for the starting point of the curve; this origin is not the same as that used in Fig. 10. It is seen that the curve only exists when

$$\frac{r}{R} \geqslant \sqrt{(2\mu^2-1)} = 0{\cdot}5$$

and that for any practical purpose the interface radius r_1 would have to be larger than the lower limit of $0{\cdot}5R$ and probably have a value near to μR, i.e. approximately $0{\cdot}8R$. The maximum height the lower canopy could have in this case is about $0{\cdot}3R$, which leaves little room to accommodate a load unless it is mounted on a platform or cantilevered into the upper canopy. The maximum total height for the whole structure is given with an upper-canopy radius $a = r_1 = \mu R$ which again limits the size of permissible load.

The maximum height of the lower canopy H/R for different values of $\mu > 1/\sqrt{2}$ is shown approximately in the table below.

TABLE

Values of H/R for $\mu > 1/\sqrt{2}$

$\mu = \frac{b}{R}$	$\doteq \frac{H}{R}(\delta = 0)$
0·7071	0·533
0·7473	0·467
0·8406	0·304
0·9354	0·127
0·9924	0·015

It should be remarked that from a practical point of view the part of the curve lying between $r/R = \mu$ and $r/R = 1$ can be regarded as an arc of a circle of radius $(1-\mu)$, in fact a semicircle centred at $r = \mu R$, for values of μ larger than $1/\sqrt{2}$.

It is not intended to pursue further in this Appendix the study of configurations with $\mu > 1/\sqrt{2}$: there is some doubt as to whether systems with $\mu > 1/\sqrt{2}$ could be sufficiently pressurised to reach the hovering state and the necessity of cantilevering the load, with a large μ, to get it off the ground demands the use of additional members to brace the structure and may invalidate the statical discussion of the present report. Experiment only can decide whether configurations with $\mu > 1/\sqrt{2}$ are of practical use.

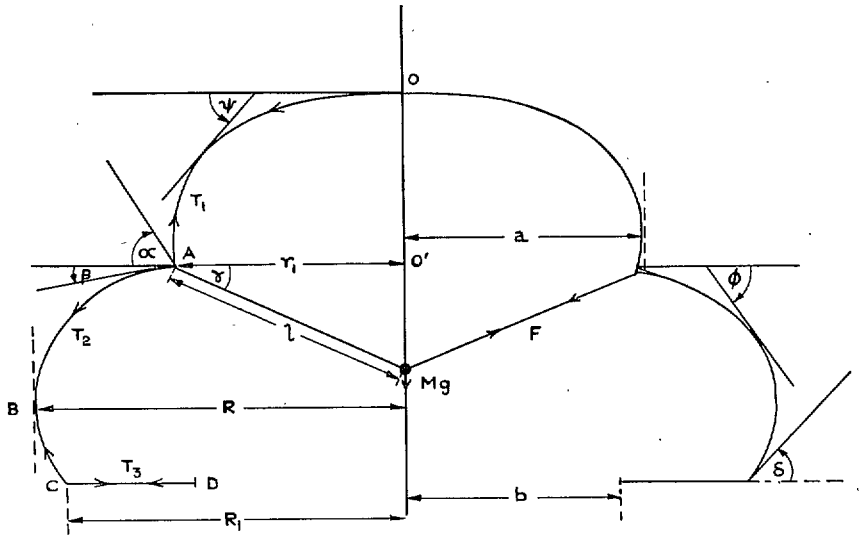

FIG. 1(i). Diagram of a lifting system showing the notation used.

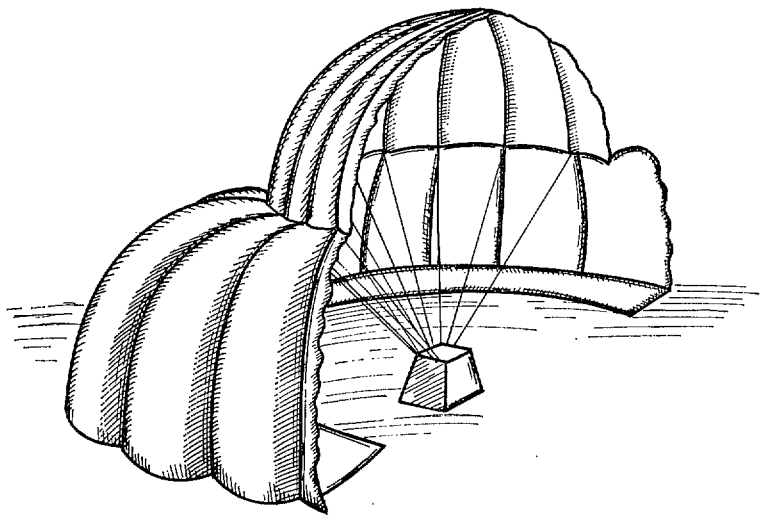

FIG. 1(ii). Sectionalised view of a lifting structure.

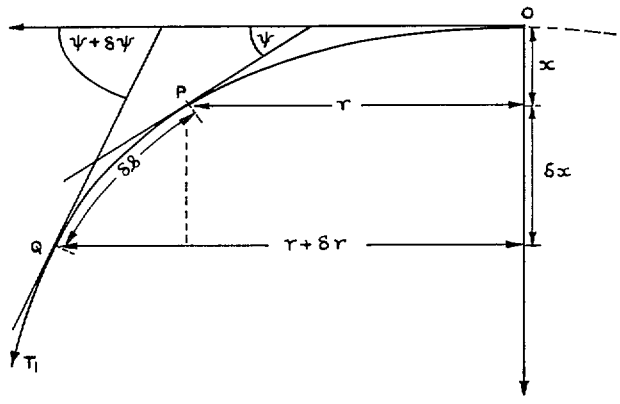

FIG. 2. A section of the upper canopy

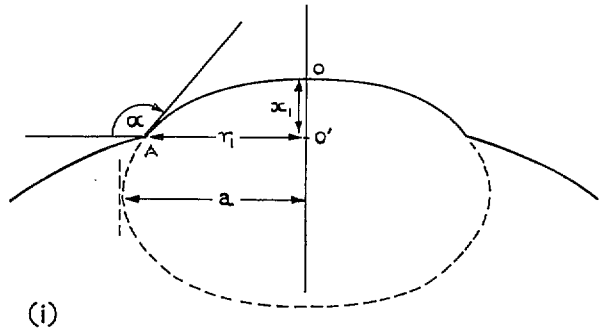

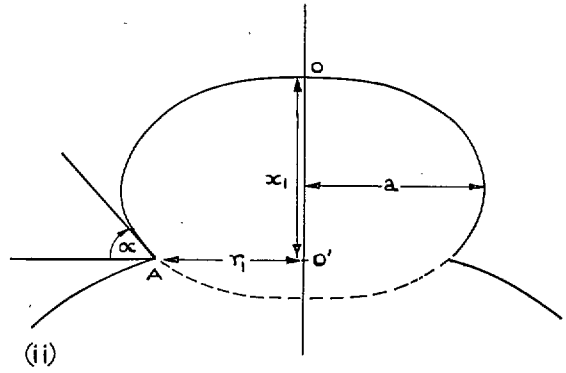

FIGS. 3(i) and (ii). Sectional forms for the upper canopy.

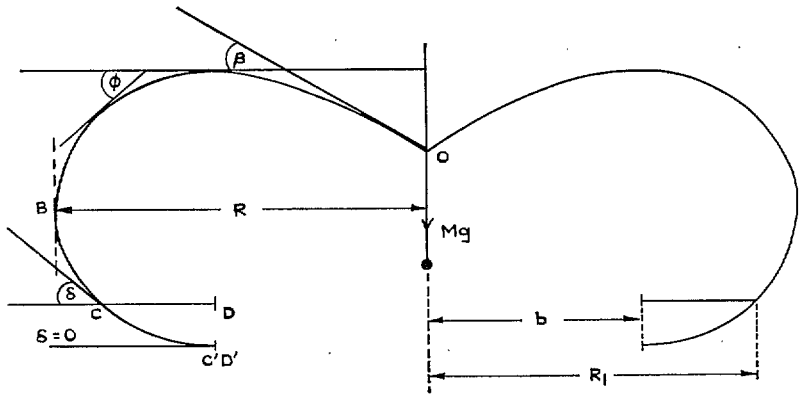

FIG. 4. Diagram of a lifting system with single-point suspension.

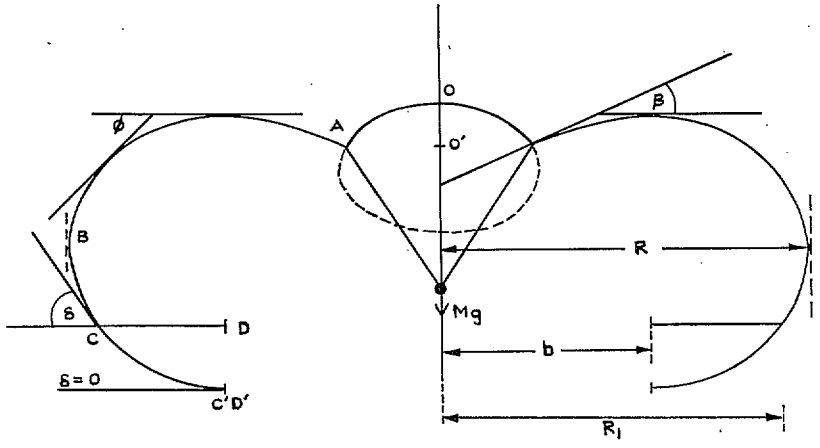

FIG. 5. A lifting system with an upper canopy and negative value of β.

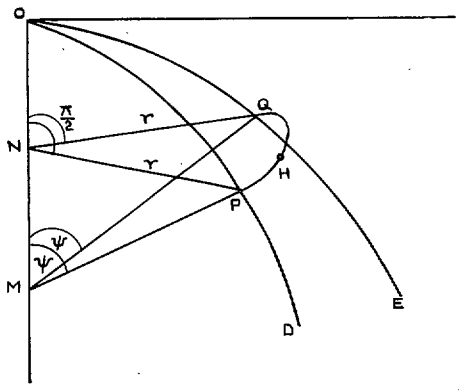

FIG. 6. Diagram showing the notation used for the gore generation.

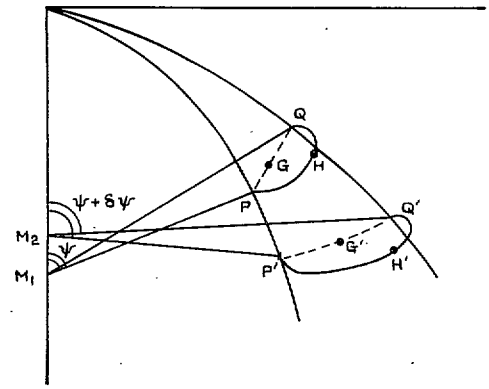

FIG. 8. Diagram showing the notation used for determining the gore length.

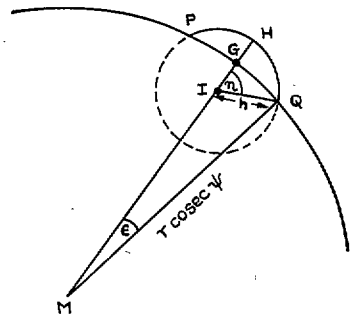

FIG. 7. Diagram showing the notation used for the gore generating circle.

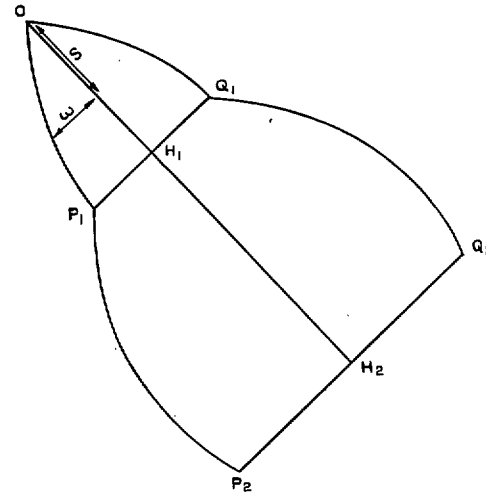

FIG. 9. The complete gore.

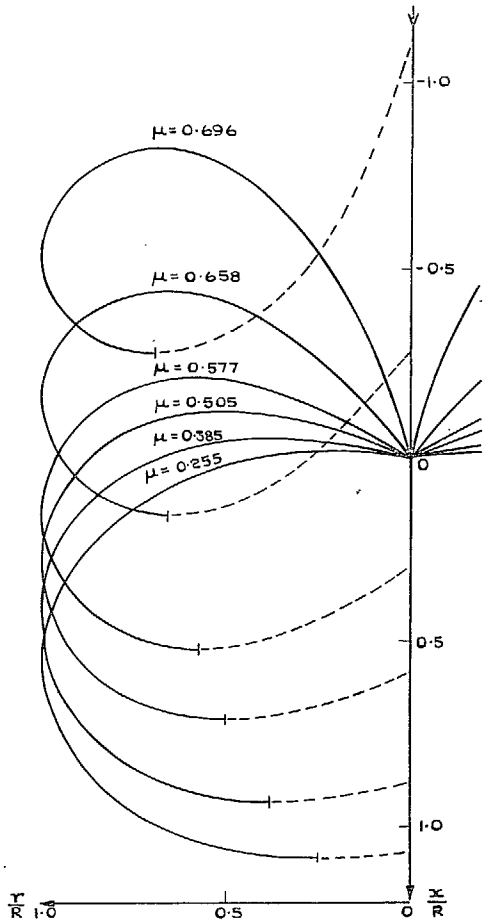

FIG. 10. Curves for the lower canopy.

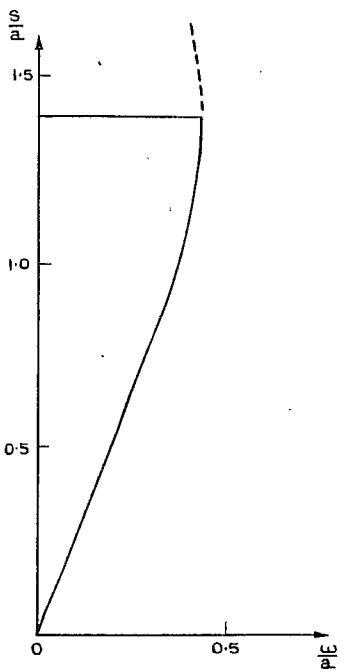

FIG. 11. An example of an upper-canopy semi-gore with $a/h = 2{\cdot}0$ and $n = 8$.

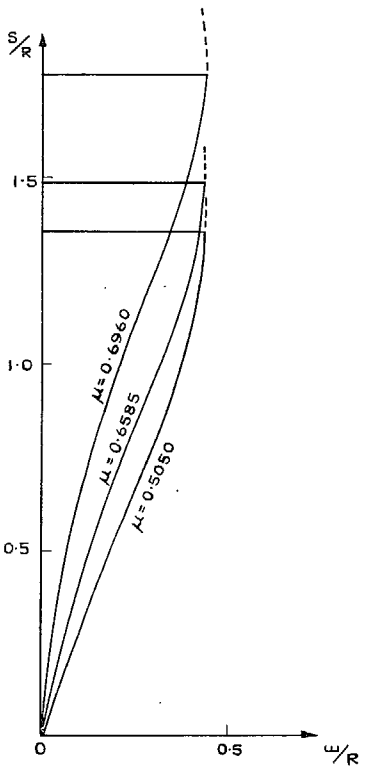

FIG. 12. Examples of the lower-canopy semi-gores for $R/h = 2{\cdot}0$; $n = 8$; $\mu = 0{\cdot}5050$, $0{\cdot}6585$ and $0{\cdot}6960$.

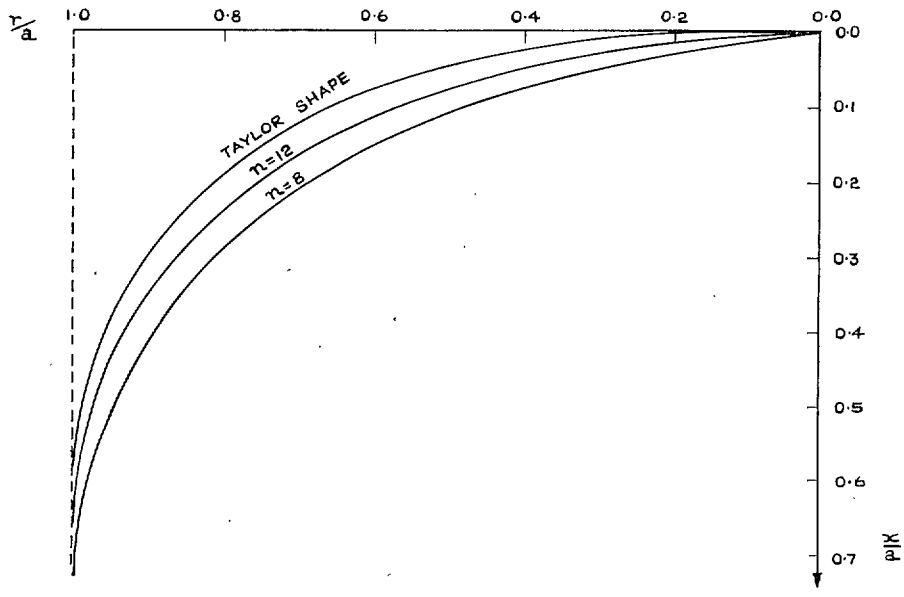

FIG. 13. Upper-canopy cord configurations for $a/h = 2{\cdot}0$ (higher approximation).

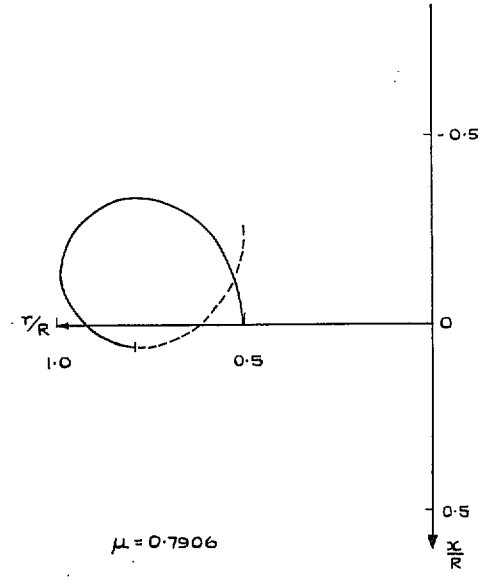

FIG. 14. Example of the lower-canopy curve for $\mu = 0{\cdot}7906 > 1/\sqrt{2}$.

(90068) Wt. 66/2301 K.5 9/64 Hw.

Publications of the Aeronautical Research Council

ANNUAL TECHNICAL REPORTS OF THE AERONAUTICAL RESEARCH COUNCIL (BOUND VOLUMES)

1942 Vol. I. Aero and Hydrodynamics, Aerofoils, Airscrews, Engines. 75*s.* (post 2*s.* 9*d.*)
Vol. II. Noise, Parachutes, Stability and Control, Structures, Vibration, Wind Tunnels. 47*s.* 6*d.* (post 2*s.* 3*d.*)

1943 Vol. I. Aerodynamics, Aerofoils, Airscrews. 80*s.* (post 2*s.* 6*d.*)
Vol. II. Engines, Flutter, Materials, Parachutes, Performance, Stability and Control, Structures. 90*s.* (post 2*s.* 9*d.*)

1944 Vol. I. Aero and Hydrodynamics, Aerofoils, Aircraft, Airscrews, Controls. 84*s.* (post 3*s.*)
Vol. II. Flutter and Vibration, Materials, Miscellaneous, Navigation, Parachutes, Performance, Plates and Panels, Stability, Structures, Test Equipment, Wind Tunnels. 84*s.* (post 3*s.*)

1945 Vol. I. Aero and Hydrodynamics, Aerofoils. 130*s.* (post 3*s.* 6*d.*)
Vol. II. Aircraft, Airscrews, Controls. 130*s.* (post 3*s.* 6*d.*)
Vol. III. Flutter and Vibration, Instruments, Miscellaneous, Parachutes, Plates and Panels, Propulsion. 130*s.* (post 3*s.* 3*d.*)
Vol. IV. Stability, Structures, Wind Tunnels, Wind Tunnel Technique. 130*s.* (post 3*s.* 3*d.*)

1946 Vol. I. Accidents, Aerodynamics, Aerofoils and Hydrofoils. 168*s.* (post 3*s.* 9*d.*)
Vol. II. Airscrews, Cabin Cooling, Chemical Hazards, Controls, Flames, Flutter, Helicopters, Instruments and Instrumentation, Interference, Jets, Miscellaneous, Parachutes. 168*s.* (post 3*s.* 3*d.*)
Vol. III. Performance, Propulsion, Seaplanes, Stability, Structures, Wind Tunnels. 168*s.* (post 3*s.* 6*d.*)

1947 Vol. I. Aerodynamics, Aerofoils, Aircraft. 168*s.* (post 3*s.* 9*d.*)
Vol. II. Airscrews and Rotors, Controls, Flutter, Materials, Miscellaneous, Parachutes, Propulsion, Seaplanes, Stability, Structures, Take-off and Landing. 168*s.* (post 3*s.* 9*d.*)

1948 Vol. I. Aerodynamics, Aerofoils, Aircraft, Airscrews, Controls, Flutter and Vibration, Helicopters, Instruments, Propulsion, Seaplane, Stability, Structures, Wind Tunnels. 130*s.* (post 3*s.* 3*d.*)
Vol. II. Aerodynamics, Aerofoils, Aircraft, Airscrews, Controls, Flutter and Vibration, Helicopters, Instruments, Propulsion, Seaplane, Stability, Structures, Wind Tunnels. 110*s.* (post 3*s.* 3*d.*)

Special Volumes

Vol. I. Aero and Hydrodynamics, Aerofoils, Controls, Flutter, Kites, Parachutes, Performance, Propulsion, Stability. 126*s.* (post 3*s.*)
Vol. II. Aero and Hydrodynamics, Aerofoils, Airscrews, Controls, Flutter, Materials, Miscellaneous, Parachutes, Propulsion, Stability, Structures. 147*s.* (post 3*s.*)
Vol. III. Aero and Hydrodynamics, Aerofoils, Airscrews, Controls, Flutter, Kites, Miscellaneous, Parachutes, Propulsion, Seaplanes, Stability, Structures, Test Equipment. 189*s.* (post 3*s.* 9*d.*)

Reviews of the Aeronautical Research Council

1939–48 3*s.* (post 6*d.*) 1949–54 5*s.* (post 5*d.*)

Index to all Reports and Memoranda published in the Annual Technical Reports

1909–1947 R. & M. 2600 (out of print)

Indexes to the Reports and Memoranda of the Aeronautical Research Council

Between Nos. 2351–2449	R. & M. No. 2450	2*s.* (post 3*d.*)
Between Nos. 2451–2549	R. & M. No. 2550	2*s.* 6*d.* (post 3*d.*)
Between Nos. 2551–2649	R. & M. No. 2650	2*s.* 6*d.* (post 3*d.*)
Between Nos. 2651–2749	R. & M. No. 2750	2*s.* 6*d.* (post 3*d.*)
Between Nos. 2751–2849	R. & M. No. 2850	2*s.* 6*d.* (post 3*d.*)
Between Nos. 2851–2949	R. & M. No. 2950	3*s.* (post 3*d.*)
Between Nos. 2951–3049	R. & M. No. 3050	3*s.* 6*d.* (post 3*d.*)
Between Nos. 3051–3149	R. & M. No. 3150	3*s.* 6*d.* (post 3*d.*)

HER MAJESTY'S STATIONERY OFFICE

from the addresses overleaf

Printed and published by
HER MAJESTY'S STATIONERY OFFICE

To be purchased from
York House, Kingsway, London W.C.2
423 Oxford Street, London W.1
13A Castle Street, Edinburgh 2
109 St. Mary Street, Cardiff
39 King Street, Manchester 2
50 Fairfax Street, Bristol 1
35 Smallbrook, Ringway, Birmingham 5
80 Chichester Street, Belfast 1
or through any bookseller

Printed in England

R. & M. No. 3377

S.O. Code No. 23–3377